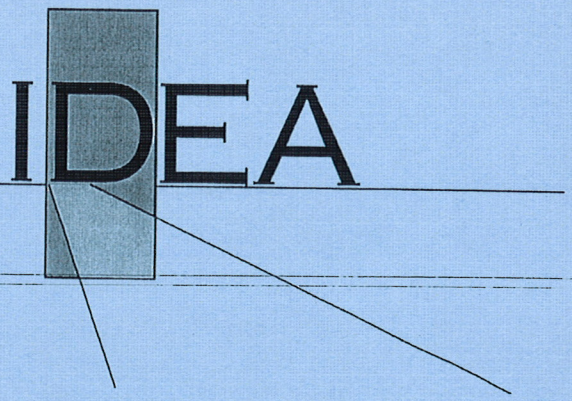

Innovations Deserving
Exploratory Analysis Programs

Highway IDEA Program

Initiation of Definitive Field Verification of Torsional Cylindrical Impulse Shear Test

Final Report for Highway IDEA Project 82

Prepared by:
Wanda Henke,
Dynamic In Situ Geotechnical Testing, Inc., Baltimore, MD

August 2003

TRANSPORTATION RESEARCH BOARD
OF THE NATIONAL ACADEMIES

INNOVATIONS DESERVING EXPLORATORY ANALYSIS (IDEA) PROGRAMS
MANAGED BY THE TRANSPORTATION RESEARCH BOARD (TRB)

This NCHRP-IDEA investigation by Dynamic In Situ Geotechnical Testing, Inc. was completed as part of the National Cooperative Highway Research Program (NCHRP). The NCHRP-IDEA program is one of the four IDEA programs managed by the Transportation Research Board (TRB) to foster innovations in highway and intermodal surface transportation systems. The other three IDEA program areas are Transit-IDEA, which focuses on products and results for transit practice, in support of the Transit Cooperative Research Program (TCRP), Safety-IDEA, which focuses on motor carrier safety practice, in support of the Federal Motor Carrier Safety Administration and Federal Railroad Administration, and High Speed Rail-IDEA (HSR), which focuses on products and results for high speed rail practice, in support of the Federal Railroad Administration. The four IDEA program areas are integrated to promote the development and testing of nontraditional and innovative concepts, methods, and technologies for surface transportation systems.

For information on the IDEA Program contact IDEA Program, Transportation Research Board, 500 5th Street, N.W., Washington, D.C. 20001 (phone: 202/334-1461, fax: 202/334-3471, http://www.nationalacademies.org/trb/idea)

Abbreviations/Acronyms

ASCE = Am. Soc. of Civil Engineers
ASTM = Am. Soc. for Testing and Materials
AU = Auburn Univ.
Bh = Borehole
BSSA = *Bulletin of the Seismological Soc. of Am.*
CPT = cone penetration test
DOT = Dept. of Transportation
EERI = Earthquake Engineering Research Inst.
EPRI = Electric Power Research Inst.
FHWA = Fed. Highway Administration
IDEA = Innovations Deserving Exploratory Analysis
I-10 = I-10/La Cienega Blvd. undercrossing
NAS = Nat. Academy of Sciences
NIST = Nat. Inst. of Standards and Technology
NSF = Nat. Science Foundation
SCT = seismic crosshole test
SPT = standard penetration test
TCIST = torsional cylindrical impulse shear test
TI = Treasure Island
UM = Univ. of Massachusetts

Symbols/Nomenclature

D = equivalent viscous damping ratio
G = secant shear modulus
G_{max} = low strain shear modulus (same as G_o)
G_o = low strain shear modulus (same as G_{max})
$G_{\gamma=0.5\%}$ = secant shear modulus for shear strain of 0.5%
R = parameter of Ramberg-Osgood equations
T = applied torque
t = time
u = porewater pressure
v_s = low strain shear wave velocity
γ = shear strain
γ_{max} = maximum test shear strain (defined on p. 2)
$\gamma_{max\ p\text{-}p}$ = peak to peak maximum test shear strain (defined on p. 2)
θ = angular displacement about longitudinal axis of probe
θ_o = angular displacement of instrumented head of probe about longitudinal axis of probe
$\bar{\sigma}_{vo}$ = vertical effective stress before porewater pressures develop
τ = shear stress
τ_{ref} = parameter of Ramberg-Osgood equations

Summary

Introduction

Herein, we report on the main elements of a coordinated 2001-02 IDEA/FHWA-led pooled-fund project. The project bears immediately on the engineering of critical constructed facilities (highway bridges and energy facilities, for example) to resist earthquakes and other dynamic loads. The main technical objectives of the project were to carry out a field testing program of the torsional cylindrical impulse shear test and to interpret the results of the program. The "impulse shear test" is a new in situ geotechnical testing method that our firm is developing. The program was to initiate a definitive field verification of this technology. The verification is to be a major step toward bringing the impulse shear test to practice.

Impulse Shear Test

In Situ Nonlinear Inelastic Shearing Deformation Characteristics—The impulse shear test was originally intended to provide, for soil deposits that may support constructed facilities, detailed information on in situ nonlinear inelastic shearing deformation characteristics. Such information is needed for earthquake engineering analysis procedures used to predict the behaviors, during earthquakes, of soil deposits (motions and occurrences of liquefaction and related deformations) and supported facilities (motions and member forces). The impulse shear test addresses the well-known problem of obtaining this information without disturbing in situ conditions excessively. Disturbances can create a great deal of uncertainty that can lead to costly, overly conservative or unconservative designs for constructed facilities. Reducing disturbances will result in greater safety, economy, and reliability of such facilities.

In Situ Resistances to Liquefaction and Related Deformations—Additionally, unexpected findings suggest that the impulse shear test may possibly be able to provide reasonably precise indications of in situ resistances of soils to liquefaction (and related deformations). In this case, the test could be used to provide estimates of liquefaction resistance without refined analysis. This potential capability was the focus of the IDEA/FHWA project.

Outcome of Project

Overall, the project was successful. We carried out a meaningful impulse shear testing program at the National Geotechnical Experimentation Site on Treasure Island in the San Francisco Bay. The program was conducted using a field prototype impulse shear testing system that we designed and constructed for FHWA. This system had shown promise in preliminary field tests. We conducted impulse shear tests in a highly relevant two layer soil sequence consisting of saturated loose sandy soils overlying a medium-stiff clay. Such a sequence has been extraordinarily hazardous during past earthquakes; the clay tends to amplify ground motions greatly and the loose sandy soils tend to liquefy. We obtained a wealth of primary test data, our interpretations of test results appear reasonable, and we addressed all the main issues we had planned to address. However, due to the malfunctions of certain newly developed prototype components, we did not obtain various refined secondary test data we had sought to obtain. These were not abnormal difficulties and much of the new equipment we added functioned effectively.

Conclusions

Our results suggest that the impulse shear test

1) is a viable means for estimating in situ nonlinear inelastic shearing deformation characteristics of soil deposits;
2) is a promising technology for providing reasonably precise indications of in situ resistances of soils to liquefaction; and
3) will be highly usable, efficient, reliable, robust, and economical when adapted for production use.

Near-Term Future Work

With the impulse shear test continuing to show promise, we feel that further work toward the introduction of the test into practice and toward the development of the test would be of value. Near-term work that logically follows the subject project includes

1) the development and manufacture of a field prototype production impulse shear testing system that is highly usable, efficient, reliable, robust, and economical;
2) the addition to the impulse shear test of the capability to measure porewater pressures; and
3) the continuation of the definitive field verification of the impulse shear test initiated by the project.

Acknowledgments

The subject project was supported by an IDEA contract (no. NCHRP-82) and by an FHWA-led pooled-fund project whose participants include FHWA and the Indiana and Mississippi state DOTs. We greatly appreciate this support. In particular, we are grateful to I. Jawed of NAS, A. DiMillio of FHWA, and R. Trent, formerly of FHWA, for all their efforts on our behalf. We also wish to express our gratitude to the members of the IDEA expert review panel for their efforts toward the project. The panel consisted of J. Cuthbertson of the Washington State DOT, A. DiMillio, H. Ghasemi of FHWA, S. Green of TerraTek, and, until his recent retirement, R. Trent. Moreover, we are appreciative of all the efforts put forth toward establishing and maintaining the National Geotechnical Experimentation Sites. Effective evaluative field testing of the impulse shear test would not have been possible without these sites.

With respect to the testing program we carried out at the Treasure Island site as part of the project, we thank Richard Faris of the Naval Facilities Engineering Command and Marianne Connoro of the City of San Francisco for their efforts toward making the program possible. And we are grateful to the City of San Francisco for allowing us to conduct impulse shear tests at this site and to the City of San Francisco Fire Station on Treasure Island for accommodating our testing program and for its hospitality. We are also deeply appreciative of Robert Greguras of HEW Drilling Company located in Palo Alto, California, for his considerable contributions to the program and to Miguel and Hugo for their help in drilling matters.

With respect to preparations for the testing program, as always, we are grateful to the Bechdon Company, Inc. of Upper Marlboro, Maryland, for the machining services it provided (often on short notice); to M. Minor of this firm for his advice and guidance on mechanical matters; and to F. Rybak of Artek Associates of Glen Arm, Maryland, for his contributions on electronic matters.

Table of Contents

Introduction

This condensed report documents the main elements of a 2001-02 IDEA project (contract no. NCHRP-82) and a portion of a complementary FHWA-led pooled-fund project. The combined project, carried out by Dynamic In Situ Geotechnical Testing, Inc., bears immediately on the engineering of critical constructed facilities (highway bridges and energy facilities, for example) to resist earthquakes and other dynamic loads. The overall objective of the project was to initiate a definitive field verification of the torsional cylindrical impulse shear test ("impulse shear test"). The impulse shear test is a new in situ geotechnical test that our firm is developing (17; see App. A) (18) (20). The verification is to help toward bringing this technology to practice. In the following sections, we provide a background, a discussion of the main elements of the project, references, and appendices.

Background

Impulse Shear Test

Nonlinear Inelastic Shearing Deformation Characteristics—The impulse shear test provides, for soil deposits, detailed information on in situ nonlinear inelastic shearing deformation characteristics needed for dynamic geotechnical earthquake engineering analysis procedures [for example, CHARSOIL, DESRA, and SHAKE (4)]. The information includes idealized nonlinear inelastic shear stress vs strain curves (τ vs γ; to date, for the strain range of 0.001 – 2.5%); low strain shear moduli (G_o); and normalized secant shear modulus reduction and equivalent viscous damping ratio curves (G/G_o and D vs γ). The analysis procedures of interest are used in the engineering of constructed facilities to predict the behaviors of soil deposits (motions and occurrences of liquefaction and related deformations) and supported facilities (motions and member forces) during earthquakes.

Resistances to Liquefaction and Related Deformations—Unexpected findings of ours suggest that the impulse shear test may have the potential for providing reasonably precise indications of the in situ resistances of soils to liquefaction and related deformations. In this case, the test would be used to provide estimates of liquefaction resistance without refined analysis. The subject project focused on this latter capability.

Problem Addressed—The general problem addressed by the impulse shear test is predicting reliably, for engineering and land use planning purposes, the behaviors of soil deposits (and supported facilities) during earthquakes. The behaviors of softer deposits in particular have contributed greatly to a broad range of losses (catastrophic to subtle but costly and disruptive) during a number of modern earthquakes. The 1985 Mexico (2) (37), 1989 Loma Prieta (10) (28), and 1995 Great Hanshin (11) earthquakes provide striking examples. Transportation facilities, most notably freeway overpass structures, have been especially vulnerable. It is widely held that an important aspect of predicting the behaviors of soil deposits reliably is estimating in situ soil characteristics. Many truly significant advances have been made in geotechnical testing technology for estimating in situ soil characteristics that bear on behaviors during earthquakes (1) (24) (29) (40); however, further progress is still needed in various areas (29). The impulse shear test addresses the well-known problem of obtaining the information of interest without disturbing in situ conditions excessively. Disturbances can create considerable uncertainty in predictions of behaviors. This uncertainty can translate into unconservative, or costly, overly conservative designs for constructed facilities.

Near-Term Potential Impact—Improving the ability to estimate in situ nonlinear inelastic shearing deformation characteristics for soil deposits will lead to more effective earthquake

engineering and, in turn, to greater safety, economy, and reliability of critical constructed facilities. These benefits will be compounded significantly if the impulse shear test is found to be capable of providing improved indications of in situ resistances to liquefaction.

Basic Idea—The impulse shear test aims to combine attractive features of existing geotechnical testing methods in a highly usable, efficient, reliable, robust, and economical manner. As in laboratory tests on soil samples recovered from sites, shearing loads that are reasonably consistent with those commonly assumed in earthquake analyses are applied to an element of soil. The behavior of the test soil appears to correspond closely to what is thought to be behavior during earthquakes. Detailed information is provided. Tests, however, are conducted in situ with many steps being taken to preserve in situ conditions and simplicity.

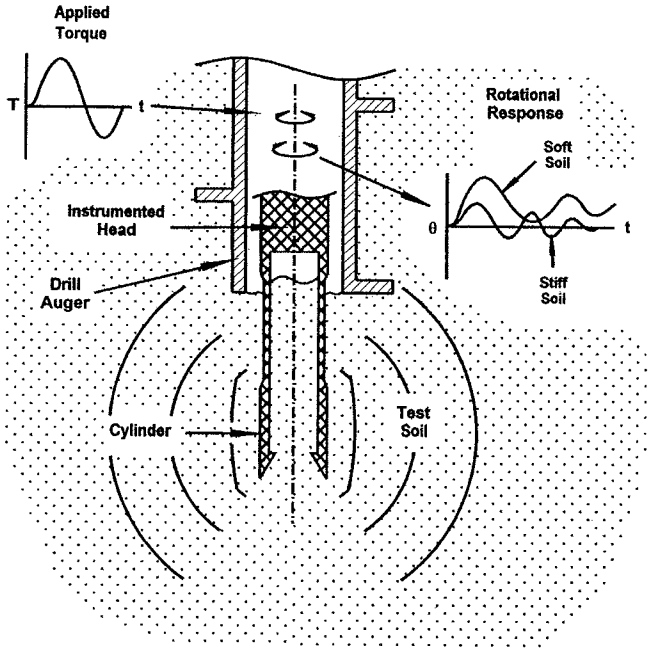

Figure 1: Main elements of field impulse shear test.

Figure 1 shows, schematically, the main elements of the field impulse shear test. An open-ended cylinder (diam. ~ 7 cm) attached to the lower end of a wireline probe is carefully penetrated into the soil below the base of a borehole/drilling auger assembly. The test soil surrounds the outside of the lower portion of the cylinder. In a single test, an impulsive torque of a selected level [expressed in volts, V (21)] is applied, through an instrumented head, to the cylinder to induce shear stresses and strains in the test soil. The cylinder responds by rotating dynamically in a manner that is strongly dependent on the nonlinear inelastic shearing deformation characteristics of the test soil. These characteristics are inferred from applied torque and angular acceleration measurements (made at the instrumented head) by simulating tests analytically.

A series of such tests is conducted at a given depth. Normally, to minimize effects of test-related disturbances, low strain tests, conducted using low levels of loading (5V excitation), are carried out first. Low strain soil characteristics are estimated from these. The low strain tests are followed by both moderate-load (10-30V, depending on soil type) and high-load (50V) high strain tests. [Herein, "high strain" refers to any level of strain for which shear stress vs strain curves are noticeably nonlinear (normally > ~0.001%).] High strain soil characteristics are estimated from the moderate-load high strain tests and "maximum test shear strains" are estimated from the high-load high strain tests. The maximum test shear strains, γ_{max}, are the maximum strains developed in the tested soils along the wall of the probe cylinder during such tests.

Interpreting Test Results—Reference 17 (see App. A) describes in some detail the evolving process of inferring the soil characteristics of interest from test results. In summary, to interpret the results of a particular low or moderate-load high strain test, an analytical axisymmetric probe-soil model such as that shown in Fig. 2 is constructed. The model is simple, yet descriptive. The torque measured in the test is applied to the modeled instrumented head. The angular acceleration of the instrumented head (among other things) is computed. A number of

such simulations are carried out (roughly 7-9), each with different soil characteristics. The characteristics resulting in the most favorable agreement, determined by a "least squares" difference method, between the measured and computed angular accelerations of the instrumented head ("most representative simulation") are considered to be representative of the characteristics of the test soil. Using the characteristics inferred from the results of the low strain and moderate-load high strain tests, high-load high strain tests are simulated to provide computed values of maximum test shear strains.

The key element of the probe-soil model is the modeling of the nonlinear inelastic shearing deformation characteristics of the test soil. We use Ramberg-Osgood equations for this. These equations are discussed in detail in Refs. 17 (see App. A), 23, and 30. The equations describe idealized nonlinear inelastic shear stress vs strain curves such as those shown in Fig. 2. Currently, the main product of a series of impulse shear tests conducted at a single test depth is a set of values for the parameters of the Ramberg-Osgood equations (G_o, τ_{ref}, and R) that result in representative idealized shear stress vs strain curves. Also, related equations may be used to obtain corresponding idealized normalized secant shear modulus reduction and equivalent damping ratio curves.

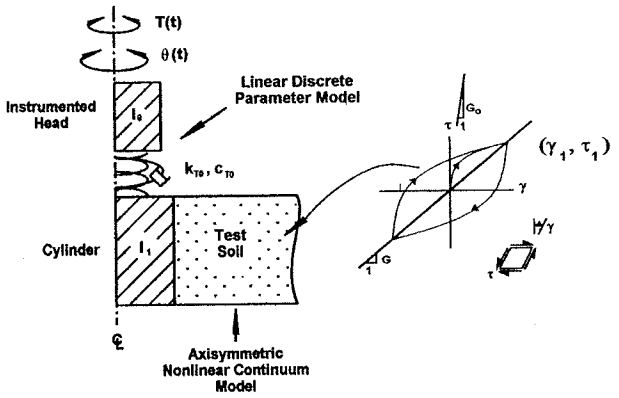

Figure 2: Analytical axisymmetric probe-soil model for simulating impulse shear tests. I_i is the mass moment of inertia of the ith mass, k_{T0} is torsional stiffness, and c_{T0} is the torsional damping coefficient, each about the longitudinal centerline.

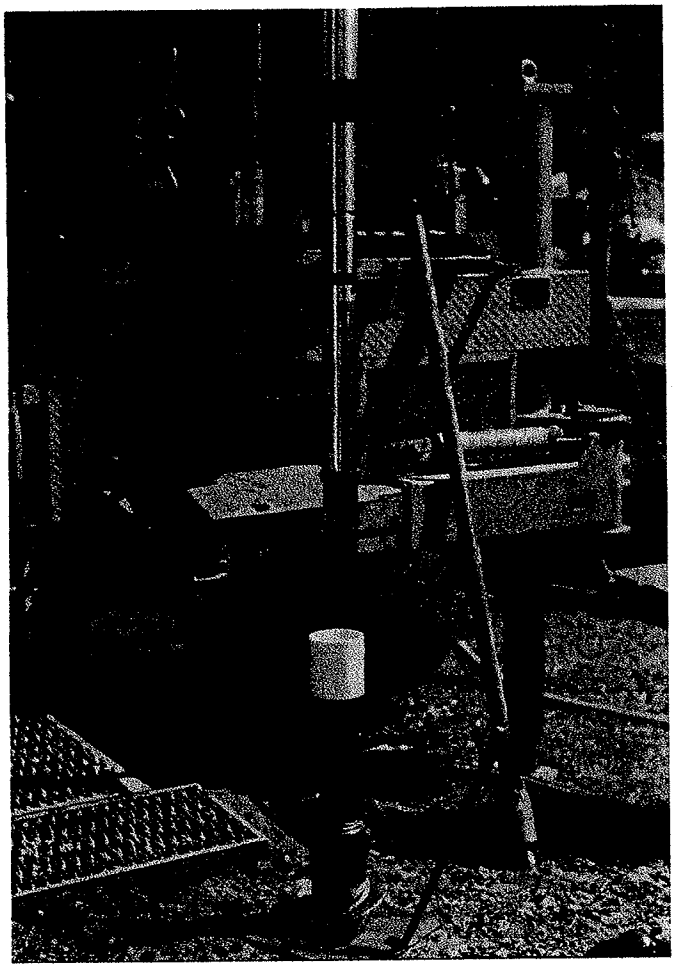

Figure 3: Probe cylinder of FHWA's field prototype impulse shear testing system.

Probe Cylinders—The probe cylinder is the most critical component of an impulse shear testing system. Figure 3 shows a photograph of a probe cylinder of a field prototype impulse shear testing system we constructed for FHWA. The cylinder, which is detachable, includes several important features, most to avoid excessive disturbances to in situ conditions. The cylinder is precisely machined and its penetrating edge is beveled to minimize disturbances during penetration (see Fig. 4). The outer, "active surface" of the cylinder is grooved longitudinally to reduce slip during

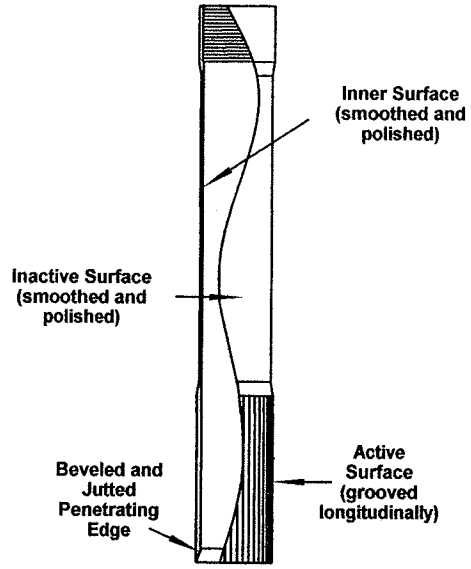

Figure 4: Probe cylinder; length of active surface = 15.2 cm, length of inactive surface = 27.9 cm, and diameter = 7.0 cm.

testing. So that tests are conducted only on deeper, less disturbed soil, the upper portion of the cylinder is machined to a radius somewhat less than that of the roots of the grooves and smoothed and polished to provide an "inactive surface" that does not grip the soil. To minimize the influence of the soil within the cylinder on its motion (the soil inside the cylinder is not tested), the inner surface is smoothed and polished, soil is diverted away from the surface by a jutted penetrating edge, and confining pressure on the soil within the cylinder is minimized by providing excess volume (through added length). Also, the auger assembly is filled with drilling fluid, in part, to lubricate the smooth polished surfaces.

Preparing for and Conducting a Test Series—Preparing for a series of tests for a particular depth mainly involves drilling the borehole. For simplicity and economy, we use conventional hollow-stem augers having a relatively small inner diameter (86 mm) for drilling the borehole. The lead auger is plugged during drilling. Usually, drilling fluid of a suitable density is introduced into the auger, in part to help suppress upward movement of the soil below the auger (caused by distortion in soft clays or upward flow of water in saturated sands). With the auger assembly at the depth of interest, the plug is removed with care being taken to avoid undesirable pressure gradients that might cause this soil to rise.

To conduct a test, the probe, with an attached axial load cell, hydraulic penetration cylinder, and set of lateral clamps, is lowered on a wireline into the lead auger assembly (see Fig. 5). This equipment is then clamped to the auger and the penetration cylinder is activated. The penetration of the probe cylinder into the test soil is reacted against the auger assembly/drill truck and is controlled very carefully. To minimize damage due to hard objects, we monitor the axial force acting within the probe during penetration. Should excessive force develop, further work at the depth is abandoned. Also, as part of the subject project, we added to the probe the capability to measure the axial displacement of the probe cylinder during penetration. With the probe cylinder fully penetrated (30.5 cm into soil), the penetration force is relieved, the main body of the probe is separated slightly from the probe cylinder/instrumented head assembly, and an appropriate series of impulse shear tests is conducted. After testing, the probe cylinder is extracted from the soil, all testing equipment is removed from the auger assembly, and the plug is reinserted to allow further drilling and testing.

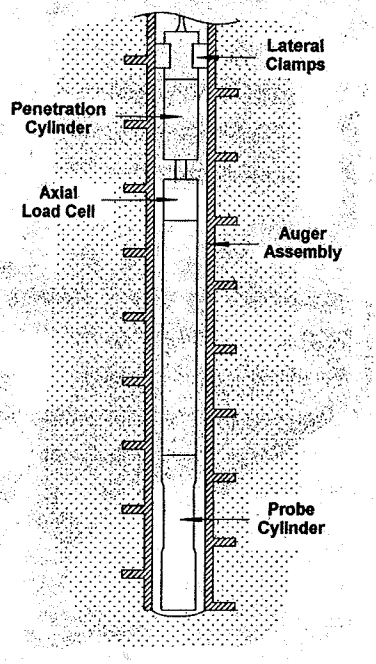

Figure 5: Probe clamped into auger assembly.

Role of Impulse Shear Test in Practice

Estimating Nonlinear Inelastic Shearing Deformation Characteristics—As a result of a unique combination of

features, the impulse shear test is expected to be applied in practice to estimating in situ nonlinear inelastic shearing deformation characteristics for soil deposits, especially when high precision is needed but cost and effort are important factors. Various in situ geotechnical testing technologies have been developed for estimating these characteristics (40). Those most comparable to the impulse shear test are a method centered on a "downhole freestanding shear device" (31); a "large-strain seismic crosshole test" (33); and the pressuremeter test (3). The first method applies to clayey soils. Basically, a cylindrical sample is carved in the soil below the base of a borehole and a strain-gaged membrane is placed over the sample. The sample is first subjected to a confining pressure and then to a torsional shear loading. Applied torque and membrane strain are measured. Using the second method, a high strain impulsive shearing disturbance is introduced into a soil deposit. Wave and particle velocities are measured using motion sensors lodged in boreholes. With the pressuremeter test, a tubular member with a concentric membrane is inserted into a soil deposit. Pressure is applied to the membrane, which expands laterally into the surrounding soil. The applied pressure and deformation of the membrane are measured. In situ nonlinear inelastic shearing deformation characteristics may be inferred from the measurements made in each of these testing methods.

The combination of features that we believe would draw interest to the impulse shear test is that the test is quite simple, compact, highly usable, robust, and efficient; applies to a broad range of relevant soil types and conditions; and provides information over strains ranging from low to reasonably high.

Estimating Resistances to Liquefaction and Related Deformations—As a result of a second unique combination of features, we believe that the impulse shear test may, ultimately, find use in providing indications of in situ resistances of soils to liquefaction when indications are needed that are particularly precise relative to those provided by more or less widely used existing in situ methods. Precise indications would be expected to be of considerable value in, for example, difficult but commonly encountered borderline cases and also costly projects. The existing methods include the SPT, the CPT, and low strain seismic tests (4). With the SPT, an opened-ended cylinder is driven into the test soil. Resistance to liquefaction is indicated by the number of hammer impacts needed to penetrate the cylinder a specified distance. In the CPT, a cone-ended cylinder is pushed continuously into the test soil. Resistance to liquefaction is indicated by the force needed to advance the cylinder. Commonly used low strain seismic tests provide measures of the travel times of low strain shear waves between, for example, motion sensors separated by known distances within soil deposits. Liquefaction resistance is indicated by the shear wave velocities calculated from these measurements.

The impulse shear test offers the following combination of features toward estimating liquefaction resistance relatively precisely: many steps are taken to reduce disturbances to the test soil (see pp. 2-4); the test applies reasonably pure shear stresses to the test soil; these stresses are of reasonably high levels; and the shear stresses result in reasonably pure shear strains. This combination of features is appealing from a fundamental standpoint. Liquefaction resistance can be strongly affected by several factors that can be easily disturbed (34); liquefaction is believed to be caused mainly by shearing loads (34); these shearing loads are generally reasonably large; and among the most visible consequences of the shearing loads are large shearing strains.

Site Investigations—Generally, in site investigations for critical facilities, impulse shear tests would be expected to complement existing methods. Impulse shear tests would be conducted to provide detailed information on the soil characteristics of interest for selected points. The locations of the impulse shear tests would be based on results from previously conducted seismic and penetration tests. These more regional tests would also be used to extrapolate the detailed information for points over the entire site. This information could, if needed, be

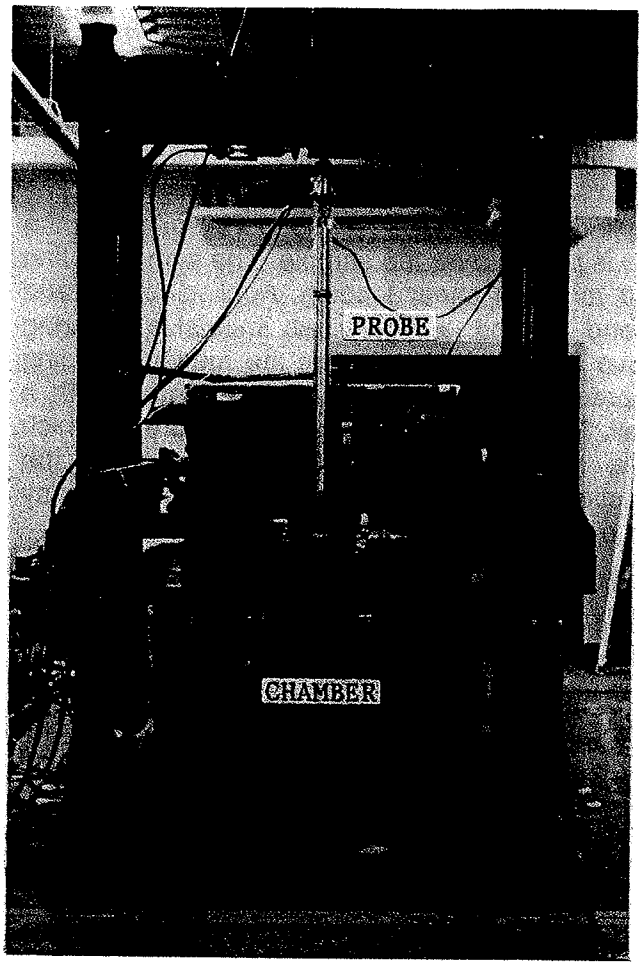

Figure 6: Exploratory testing of laboratory prototype impulse shear testing system.

extended to relevant conditions other than those in situ based on results from laboratory tests conducted on recovered samples of soil. Thus, a detailed and reasonably complete and reliable description of in situ soil characteristics needed for dynamic earthquake engineering analyses would be provided. The main intended contribution of the impulse shear tests would be to account for, to a high degree, the very important effects of in situ conditions.

Experiences with Impulse Shear Test

Our first impulse shear tests were a series of exploratory tests conducted in the laboratory on a single large sample of sand using a laboratory prototype impulse shear testing system (see Fig. 6). The results of these tests were promising and are the subject of a 1993 *Bulletin of the Seismological Society of America (BSSA)* journal article (20). Then, we conducted field impulse shear testing programs at various U.S. sites (for example, see Fig. 7) using the field prototype testing system we constructed for FHWA (see Fig. 3). The purpose of the programs was to provide preliminary evaluations of the impulse shear test with an emphasis on operability issues. The programs covered a broad range of relevant soil conditions. The impulse shear test continued to show promise and our field testing programs are summarized in a 2002 *BSSA* journal article (17; see App. A).

Main Elements of Project

Main Objectives

Our main technical objectives were to carry out field impulse shear tests at an appropriate site and to interpret the results of the tests. The project was to initiate a definitive field verification of the impulse shear test and mainly sought to

1) verify the test on its ability to provide, for selected soils that are particularly relevant to earthquake engineering, detailed information on in situ nonlinear inelastic shearing deformation characteristics;
2) address various issues that have arisen from our past preliminary field testing programs; and

3) continue the evaluation of the ability of the impulse shear test to provide reasonably precise indications of in situ resistances of soils to liquefaction and related deformations.

Main Outcome and Results

Overall, the subject project was successful. We carried out a meaningful field impulse shear testing program; our interpretations of the results from the tests of the program are reasonable; and we addressed all the main issues that we had planned to address. No major difficulties were encountered.

Field Testing Program—We carried out an impulse shear testing program during 2002 at the National Geotechnical Experimentation Site on Treasure Island in the San Francisco Bay. We conducted tests in the upper two layers of soil, shown schematically in Fig. 8. These layers are representative of a sequence that has been particularly hazardous during past earthquakes. The upper layer (~11.5 m thick) consists of sublayers of saturated loose silty sands while the underlying layer (~15 m thick) consists of medium-stiff clay. The clay layer can amplify ground motions greatly and saturated loose sandy layers can liquefy and undergo almost limitless deformations. At the Treasure Island site these two main layers are separated by a thin sand/clay transition sublayer.

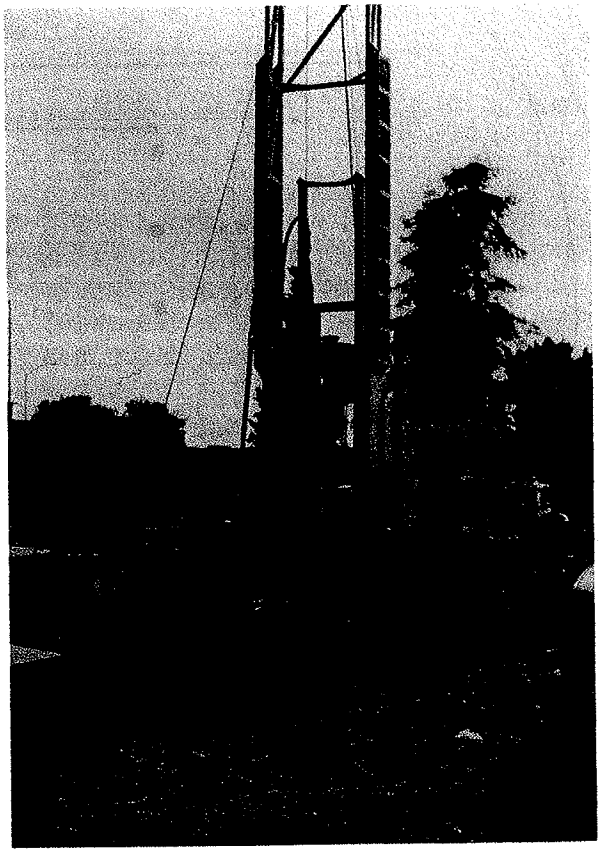

Figure 7: FHWA's field prototype impulse shear testing system prior to testing at the I-10/La Cienega Blvd. undercrossing in Los Angeles, Calif. This was the site of a freeway structure that collapsed during the 1994 Northridge earthquake.

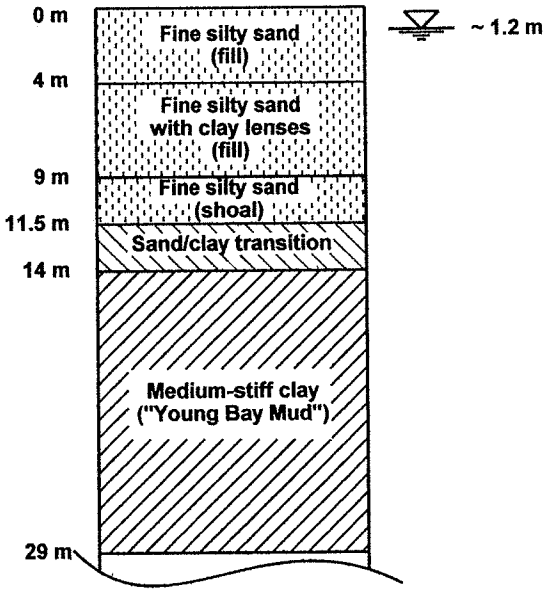

Figure 8: Relevant soil layering at the Treasure Island site. Information is based on information from Refs. 5, 6, and 14.

We had also conducted impulse shear tests at the Treasure Island site in the sandy layer in 1996 (8) (17; see App. A). In contrast to the tests of the 2002 program, these tests were of a very preliminary character. While we were able to evaluate the impulse shear test to a limited extent, our primary interest at that time was operability issues.

With respect to details of the 2002 program, impulse shear tests were carried out at 13 depths in two boreholes. The locations of the boreholes are shown in Fig. 9. We only report the results of tests conducted in borehole #1 (Bh #1) herein. The tests conducted in borehole #2 were intended to provide

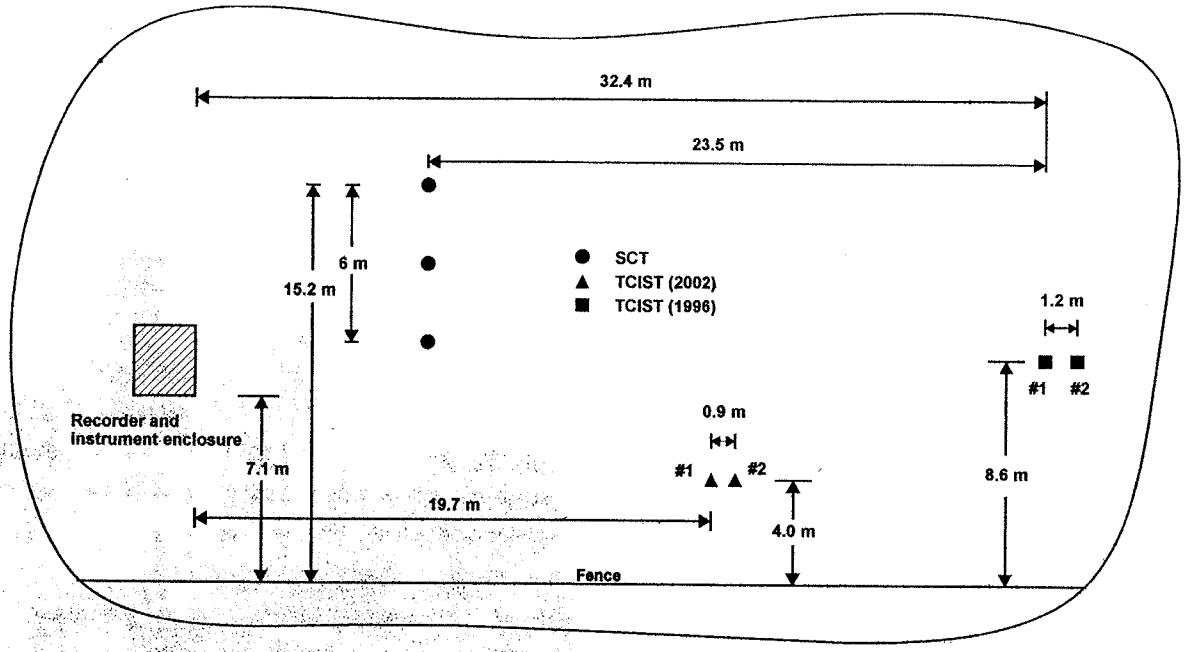

Figure 9: Plan view of tested area at the Treasure Island site. Information on array instrumentation and seismic crosshole tests (SCT) is based on information provided in Ref. 5 and by Ref. 13.

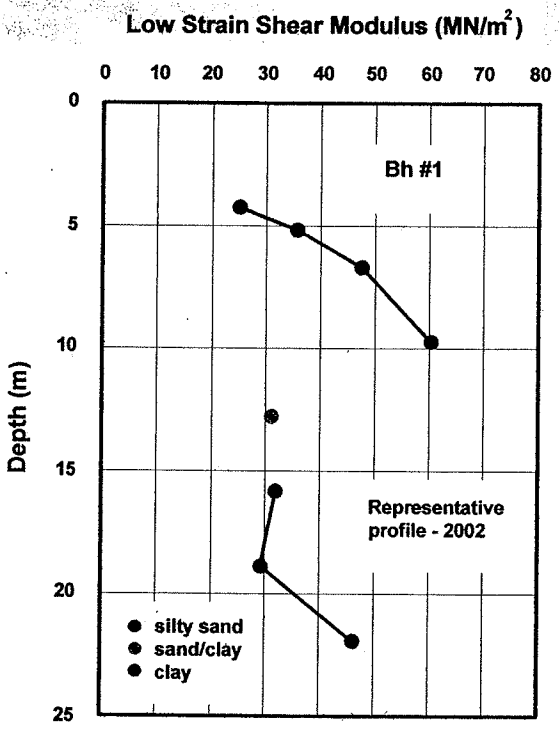

Figure 10: Low strain shear modulus profile inferred for the Treasure Island site from the results of representative impulse shear tests (2002 testing program).

rough preliminary evaluations of new proprietary equipment we activated solely for these tests and are not definitive.

We obtained all primary impulse shear test results (applied torques and angular accelerations) for 10 depths in borehole #1. (Unfortunately, we accidentally erased from computer memory all our test results for the depth of 8.23 m.) Additionally, the testing program allowed us to test many new prototype components that we had added to FHWA's impulse shear testing system as part of the subject project. We did experience technical difficulties with two of the new components that impacted our productivity and prevented us from obtaining refined secondary results (axial loads in the probe during the penetration of the probe cylinder into the tested soils and corresponding axial displacements of the piston rod of the penetration cylinder). However, these were neither major nor fundamental difficulties.

Interpretations of Test Results—In Table 1 and Figs. 10-12, we present the information we inferred from the results of the representative impulse shear tests we conducted in borehole #1. (Herein "representative" results are ones that

Depth (m)	Soil Type/Conditions*	Comments	Density+ (kg/m^3)	G_o (MN/m^2)	τ_{ref} (kN/m^2)	R	τ_{ref} (kN/m^2)	R
					without porewater pressure generation		with porewater pressure generation	
~1.2	water table							
4.27	saturated loose fine silty sand (fill)		1920	25.1	5.38	3.72	5.25	3.56
5.18	saturated clayey sandy silt (fill)		1920	35.7	10.3	3.56	10.0	3.41
6.71	saturated loose fine silty sand (fill)		1920	47.5	11.5	3.56	11.3	3.56
8.23	Saturated clayey silty sand (fill)	Test data lost						
9.75	saturated loose fine silty sand (shoal)		1920	60.4	6.59	4.03	5.25	3.41
11.3	Saturated loose fine silty sand (shoal)	High penetration rate. May have disturbed soil. 30 V and 50 V tests not interpretable.	1920	6.44	6.59	3.72		
12.8	likely, sand/clay transition		1920	31.1	16.3	3.09		
15.9	medium-stiff clay ("Young Bay Mud")		1760	31.9	22.5	2.91		
18.9	medium-stiff clay ("Young Bay Mud")	Guard ring may have interfered with test	1760	29.3	25.0	2.75		
21.9	medium-stiff clay ("Young Bay Mud")		1760	46.2	25.0	2.91		

*Descriptions based on inspections of recovered soils and available information (5) (6)
+Based on available information (6) (22)

Table 1: Soil types and conditions at the Treasure Island site and information inferred from results of impulse shear tests conducted in borehole #1 at this site (2002 testing program).

do not include the information we inferred for the test series carried out for the depth of 11.3 m. Likely, this test series was conducted improperly.) Figure 10 shows a low strain shear modulus profile; Fig. 11a presents shear stress vs strain curves (initial loading only); and Fig. 11b provides representative average (for convenience) normalized secant shear modulus reduction and damping ratio curves. These latter curves are averages of the individual curves, shown in Fig. 12, that we inferred for the depths at which we carried out representative impulse shear tests. Our interpretations of test results are based on the probe-soil model shown in Fig. 2 with $I_o = 2.72 \times 10^{-3}$ kg-m^2, $I_1 = 2.08 \times 10^{-3}$ kg-m^2, $k_{To} = 158$ kN-m/rad, and $c_{To} = 0.83$ kg-m^2/s. The value for c_{To} corresponds to a damping ratio of 0.02 for a single degree of freedom system consisting of the upper mass and the spring. Sample results are provided in Appendix B.

The results draw various observations. For example, the stress vs strain curves of Fig. 11a show a broad range of characteristics that is highly ordered. The clays show the greatest high strain shearing rigidity, the sandy soils show the least, and the sand/clay transition soil shows

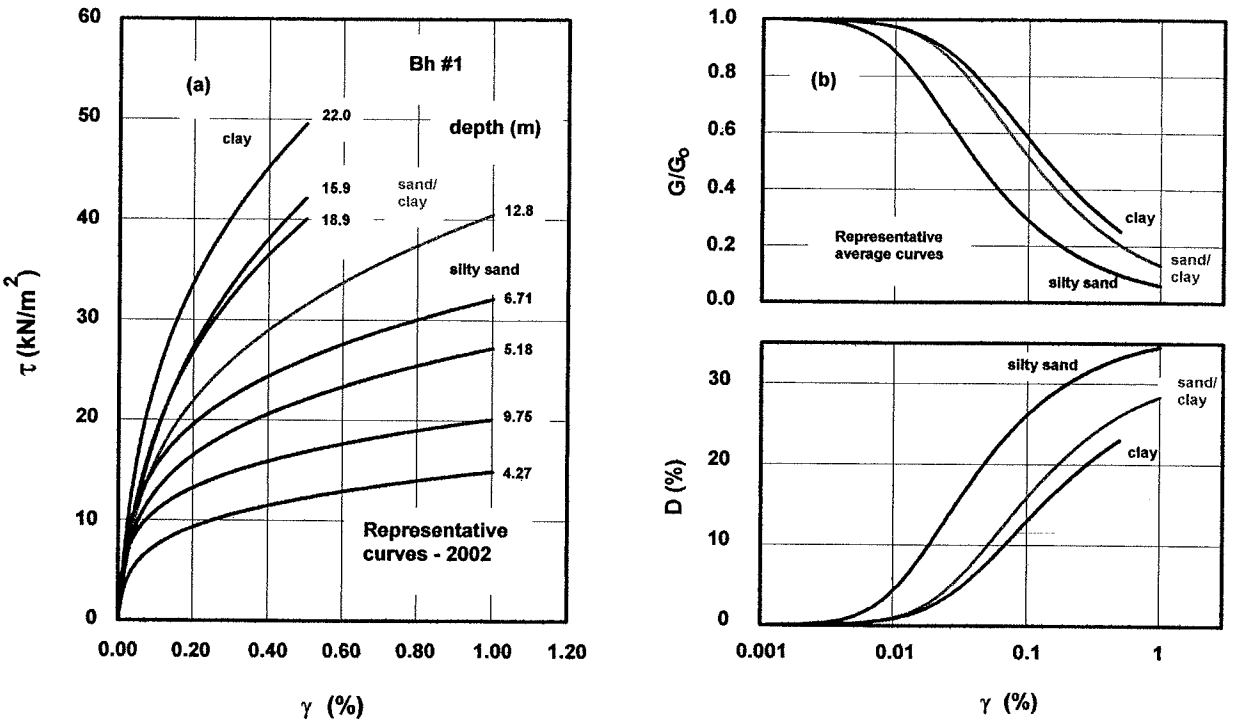

Figure 11: Idealized nonlinear inelastic shearing deformation characteristics inferred for soils of the Treasure Island site from results of representative impulse shear tests (2002 testing program).

an intermediate level. The shear modulus reduction and damping ratio curves of Fig. 11b show trends consistent with ones reported in the literature (39). For instance, the shear modulus reduction curve for the sandy soils falls below that for the clay soil. And as would be expected, the curve for the sand/clay transition falls between the two.

We should note that, in our interpretations of test results, we made three departures from our normal practices (17; see App. A). First, for convenience, we simulated entire tests but compared angular accelerations only over specified periods. Previously, we had simulated only selected portions of tests. For example, with high strain tests our practice had been to simulate the initial portions of tests during which peak strains are high. Second, we filtered low strain applied torque records using a low-pass digital filter having a cutoff frequency of 1500 Hz instead of 2500 Hz. This was to suppress a roughly 2200 Hz component of what appears to be noise. Lastly, we interpreted the low strain test results for the depth of 6.71 m by comparing the frequency spectra of the computed and measured angular accelerations of the instrumented head rather than the accelerations directly. We judged that, for this particular depth, the spectrum approach resulted in improved interpretations of test results.

Main Issues Addressed by Project

In the following subsections, we summarize the issues that have arisen in the course of our past field testing programs that were the main issues addressed by the subject project and present our findings.

Test-Related Disturbances—One fundamental issue we addressed is that of the levels of test-related disturbances and their impacts on test results. Past comparisons we have made between low-strain shear modulus/shear wave velocity profiles inferred using the impulse shear test and such profiles inferred using more established low strain seismic tests have consistently

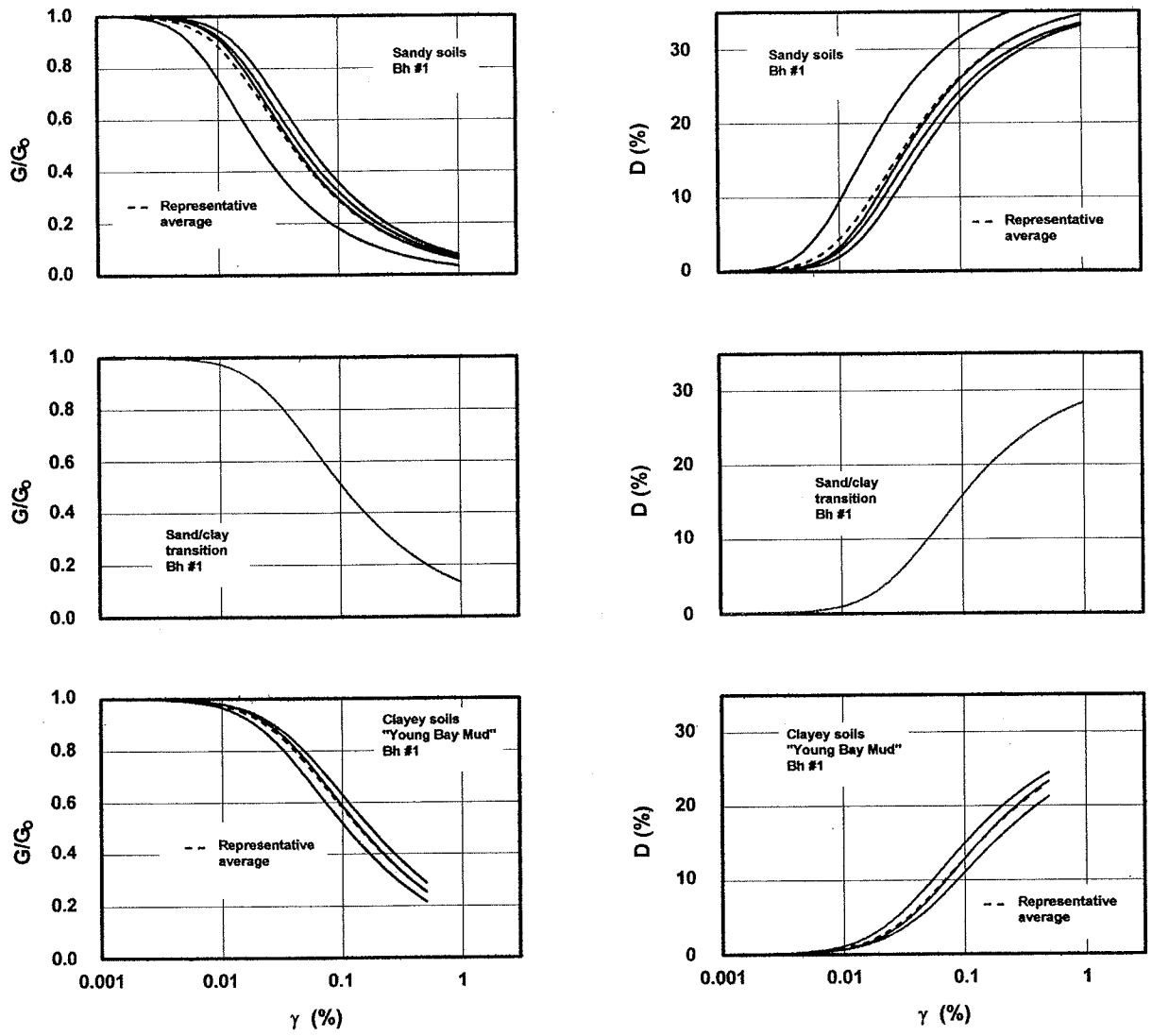

Figure 12: Representative individual idealized normalized secant shear modulus reduction and damping ratio curves inferred for soils of the Treasure Island site from results of representative impulse shear tests (2002 testing program).

shown reasonable agreements (17; see App. A). Because results from low strain seismic tests usually reflect strongly the undisturbed characteristics of soil deposits, these agreements suggest that the impulse shear test does not disturb the tested soils excessively.

Though test-related disturbances appear to have been contained, as we have pointed out (17; see App. A), our 1996 low strain results for the shallow saturated loose silty sands of the Treasure Island site suggest that test results for this site may have been impacted by drilling-related disturbances. In Fig. 13, we show a comparison between low strain shear wave velocity profiles inferred from results of the 1996 impulse shear tests and low strain seismic crosshole tests. While the profile for the impulse shear test follows closely the trend of the profile based on the seismic tests, it consistently falls somewhat below that profile. We considered various explanations (penetration-related disturbances and anisotropy within the tested soils, for example). We judged the most likely sources of the observed differences to be the very real possibility of natural variations in soil conditions [the impulse shear tests were conducted some

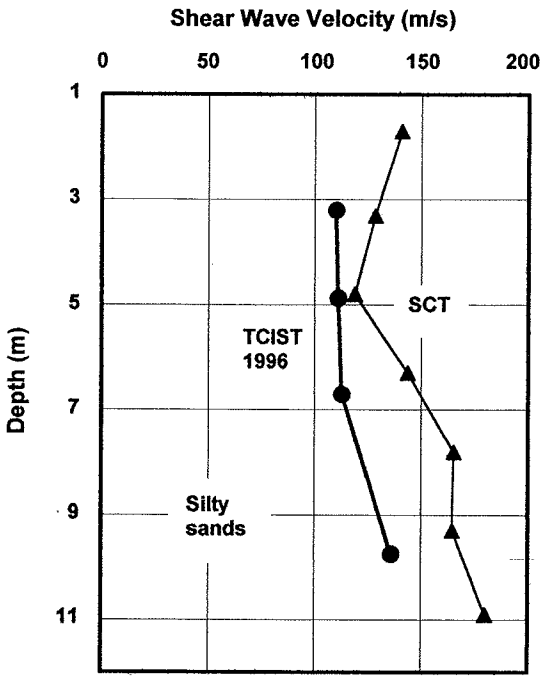

Figure 13: Low strain shear wave velocity profiles inferred for the Treasure Island site. The seismic crosshole test (SCT) profile is based on information from Refs. 5, 6, and 14.

distance from the seismic tests (8) and SPT records for the site show variability (5)] and/or small rises of fluid sand toward the auger assemblies that appeared to have occurred during the removals of the auger plug from the assemblies in preparation for testing. Such rises would be expected to reduce soil shearing stiffnesses and thus, result in underestimates in shear wave velocities.

In an effort to address this matter, we designed and had manufactured a special plug for our augers. Patents are pending on the plug. The plug, shown schematically in Fig.14, is intended to reduce the tendency of saturated soil to rise toward auger assemblies upon removal of the plug from the assemblies. Basically, the plug is to allow drilling fluid to come into contact with its lower portion immediately prior to its removal. Thus, suction forces that normally act on the soil below plugs as they are being removed, and therefore the tendency for the soil below the plug to rise, would be expected to be reduced considerably. During drilling, however, through a wedging mechanism, the plug is designed to act conventionally (as a single solid unit).

With respect to the project's findings, comparisons of information inferred from results of our 2002 Treasure Island impulse shear tests to corresponding published information inferred from results of more established tests provide continued support for the idea that disturbances induced in the tested soils by impulse shear tests are contained. Figure 15 presents a comparison between the low strain shear wave velocities we inferred as part of our 2002 testing program and ones inferred from results of seismic crosshole tests conducted at the Treasure Island site. The agreements are reasonable.

Also, the special auger plug appears to have functioned effectively. Figure 16 shows the low strain shear wave velocity profiles we inferred for the upper silty sand layer as parts of the 1996 and the 2002 testing programs along with the seismic crosshole test profile we had used in the Fig. 13 comparison (8) (17; see App. A). The profile for the 2002 testing program, in which we used the special plug, exceeds that for the 1996 program, in which we used a conventional plug, for each test depth and also shows improved agreement with the profile for the seismic crosshole tests. We do not know to what degree nonuniformities of soil characteristics affected results; the 1996 and 2002

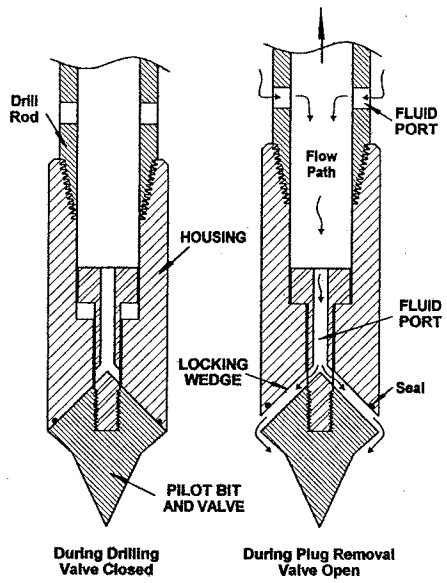

Figure 14: Special plug for lower end of auger assembly (patents pending). The plug remains fixed at the bottom of the auger assembly during drilling and rotates with the assembly.

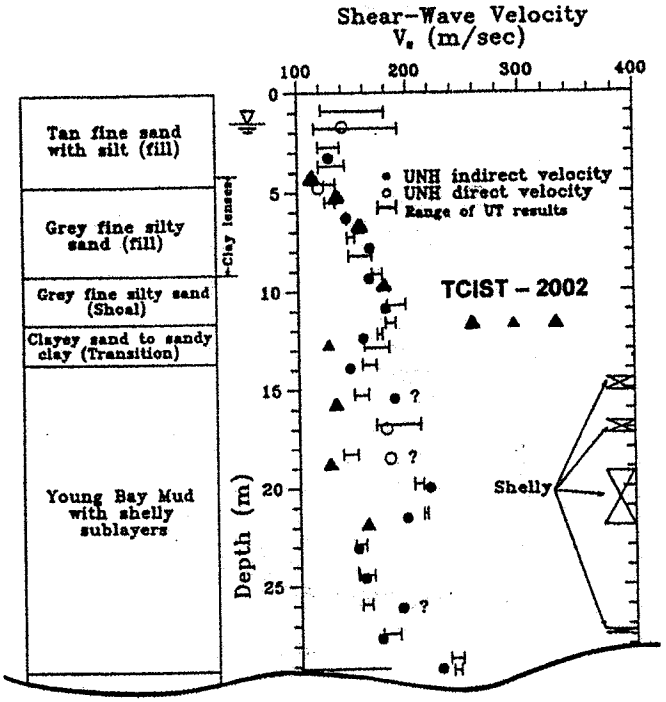

Figure 15: Low strain shear wave velocities inferred from results of representative impulse shear tests conducted at the Treasure Island site (2002 testing program) superimposed on low strain shear wave velocities inferred from results of seismic crosshole tests carried out at the site and published in Ref. 6. UNH is Univ. of New Hampshire and UT is Univ. of Texas at Austin.

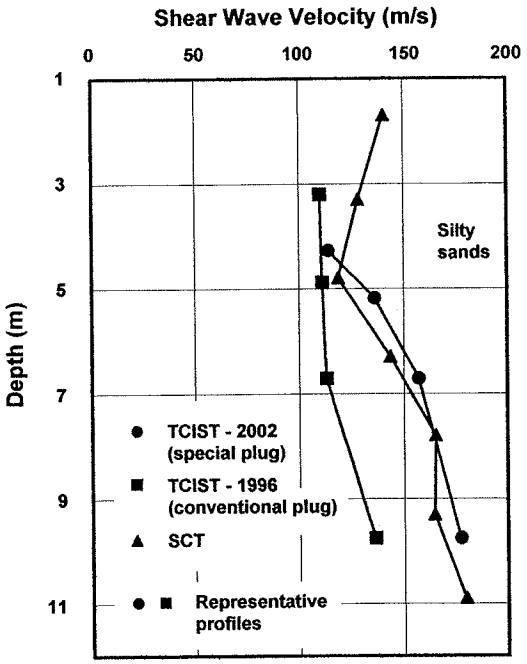

Figure 16: Low strain shear wave velocity profiles inferred for the upper silty sand layer at the Treasure Island site. The seismic crosshole test (SCT) profile is based on information from Refs. 5, 6, and 14.

programs were conducted some distance from each other (see Fig. 9).

With respect to high strain characteristics, in Fig. 17, we show the ranges of the representative shear stress vs strain curves (initial loading only) and the representative averages of the normalized secant shear modulus reduction and damping ratio curves we inferred for the silty sand layer from results of our 2002 and 1996 testing programs. These latter curves are shown superimposed on corresponding results from laboratory tests carried out on undisturbed samples of sand recovered from the Treasure Island site and also on corresponding general curves for sands. The stress vs strain curves obtained using the special auger plug (2002 testing program) differ considerably from those obtained using the conventional plug (1996 testing program), the former showing, on average, greater shearing rigidity. The agreements among the curves of Fig. 17b are reasonable, further suggesting that the impulse shear tests did not disturb the tested soils excessively. (The damping ratio curves are discussed under High Strain Damping Ratios for Saturated Sandy Soils, p. 18.) However, the results from the tests conducted using the special auger plug agree somewhat more favorably with the published results than the results from the tests conducted using a conventional plug. Assuming that nonuniformity of soil conditions did not affect test results greatly, this adds support to the idea that the special auger plug functioned as intended.

In Fig. 18, we compare the representative average normalized secant shear modulus reduction and damping ratio curves we inferred for the clay layer to corresponding curves inferred from results of laboratory tests conducted on undisturbed samples recovered from the layer and in Fig. 19, we make a similar comparison but to results from laboratory tests conducted on "San

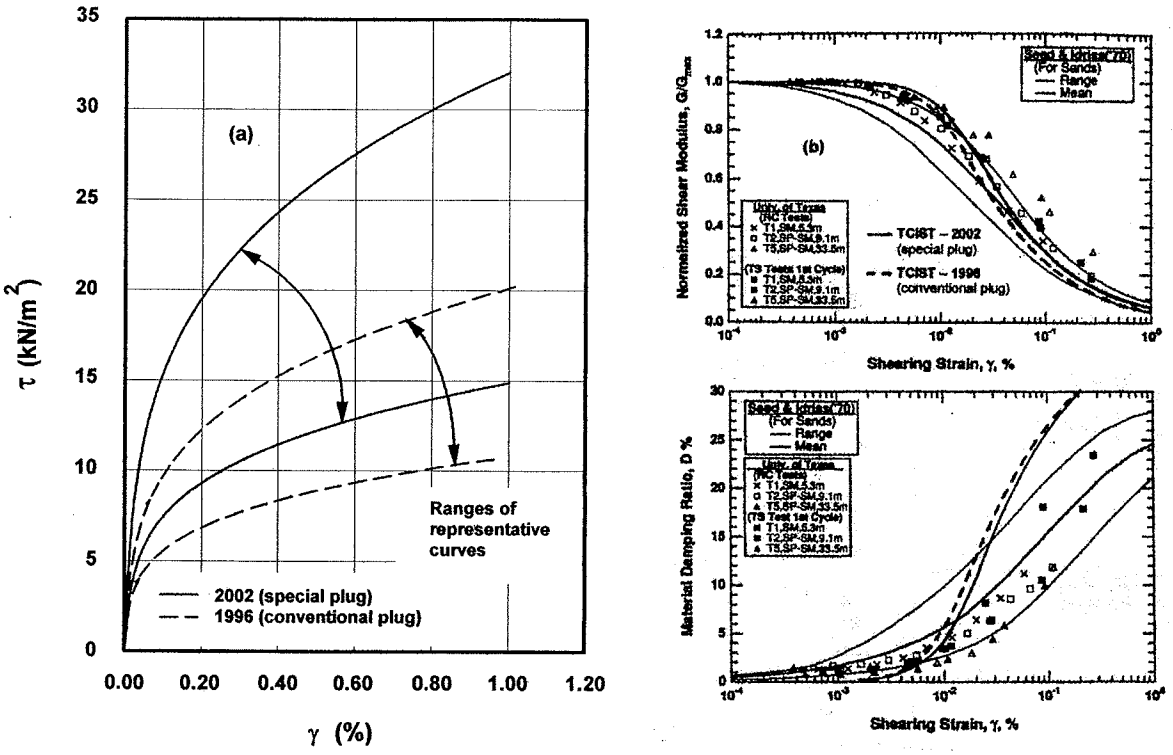

Figure 17: High strain information inferred from results of representative impulse shear tests conducted in the upper silty sand layer at the Treasure Island site. (a) Ranges of shear stress vs strain curves. (b) Normalized secant shear modulus reduction and damping ratio curves (representative average curves) superimposed on corresponding information published in Ref. 22 and based on results from laboratory resonant column (RC) and torsional shear (TS) tests conducted on undisturbed samples of sand recovered from the site. The results for the depths of 5.3 and 9.1 m are the most relevant.

Francisco Bay Mud." The agreements are reasonable, further strengthening the notion that the impulse shear test does not disturb tested soils greatly. We should note that we have not yet addressed the issue of effects of strain rate. However, we estimate, for example, that in high-load high strain impulse shear tests carried out in the clay layer, the rate of strain within the tested soils at the wall of the probe cylinder in developing a representative peak strain of roughly 0.7% was about 700%/s. The rate of strain in developing this peak strain at the representative earthquake frequency of 1 Hz would be about 3%/s. A cursory review of the results of Ref. 22, presented in Fig. 18, suggest that rate of strain effects are not large for the shallow clays at Treasure Island. This reference reports that frequencies for the torsional shear tests ranged from 0.1 to 10 Hz while frequencies for the resonant column tests ranged from 20 to 130 Hz. Interestingly, for the clay layer of interest (test depths of 18.3 m and 27.4 m), the normalized secant shear modulus reduction results obtained using the resonant column test (higher strain rate) fell below, and thus, showed lower shearing rigidity than those obtained using the torsional shear test (lower strain rate). The corresponding curve for the impulse shear test agrees more closely with the results from the torsional shear tests than with the results from the resonant column tests.

We did not make comparisons for the sand/clay transition sublayer as the testing program from which we drew comparative information did not include tests on this sublayer.

Porewater Pressures—An issue that has arisen in the testing of saturated cohesionless soils is the question of whether or not porewater pressures develop during high strain impulse shear tests (17; see App. A). We have not yet had means to establish the levels of any test-induced

porewater pressures that may develop. Depending on their levels, porewater pressures could impact our interpretations of results of tests conducted in saturated cohesionless soils.

To gain insight into this matter, we added to the soil model of our existing analysis procedure for simulating impulse shear tests (see Fig. 2 and Interpreting Test Results, p. 2) a porewater pressure generation model. The model we added is that used in the well-known earthquake site response computer program DESRA (16, 26). Finn (15) has used this model in simulating cyclic simple shear tests.

Using the porewater pressure generation model, we reanalyzed the results from the representative impulse shear tests conducted in the upper silty sand layer during the 2002 testing program. We selected values for the parameters of the model that were appropriate for a highly liquefiable soil [$C_1 = 0.56$, $C_2 = 0.71$, $m = 0.43$, $k_2 = 0.0067$, and $n = 0.62$ (25)]. Consistent with our normal practice, to interpret test results, we simulated both low strain (5V) and moderate-load high strain (30V) tests. The values we inferred for the parameters of the Ramberg-Osgood equations are included in Table 1. Using these values, we then simulated high-load high strain (50V) tests.

Samples of results from our analyses are shown in Fig. 20. This figure shows, for each of the impulse shear tests analyzed for the depth of 5.18 m, the measured applied torque; the angular acceleration of the instrumented head as measured and as computed using the values inferred for the parameters of the Ramberg-Osgood equations; the computed shear stress vs strain curves for the soil at the wall of the

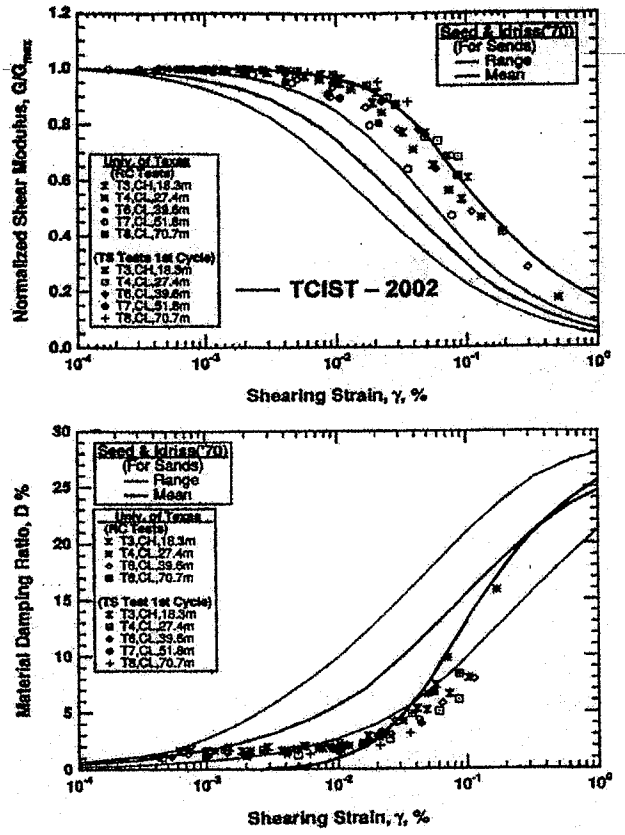

Figure 18: High strain information inferred from results of representative impulse shear tests conducted in the clay layer ("Young Bay Mud") underlying the upper silty sand layer at the Treasure Island site (representative average curves) superimposed on corresponding information published in Ref. 22 and based on results from laboratory resonant column (RC) and torsional shear (TS) tests conducted on undisturbed samples recovered from the clay layer. The results for the depth of 18.3 m are the most relevant.

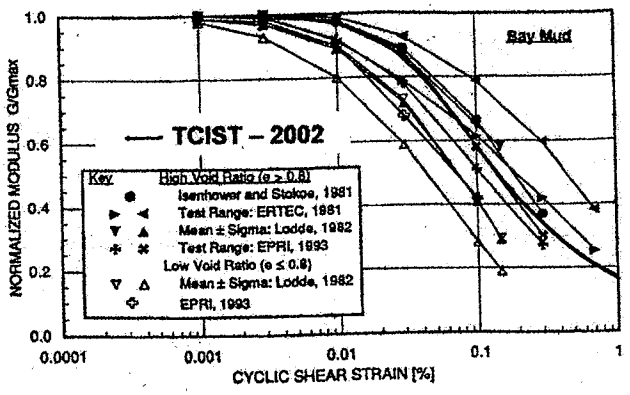

Figure 19: High strain information inferred from results of representative impulse shear tests conducted in the clay layer ("Young Bay Mud") underlying the upper silty sand layer at the Treasure Island site (representative average curve) superimposed on corresponding information published in Ref. 32 and based on results of laboratory tests conducted on samples of "San Francisco Bay Mud." The curves for high void ratios are the most relevant since the void ratios of the clay layer have been found to exceed 1.0 (22).

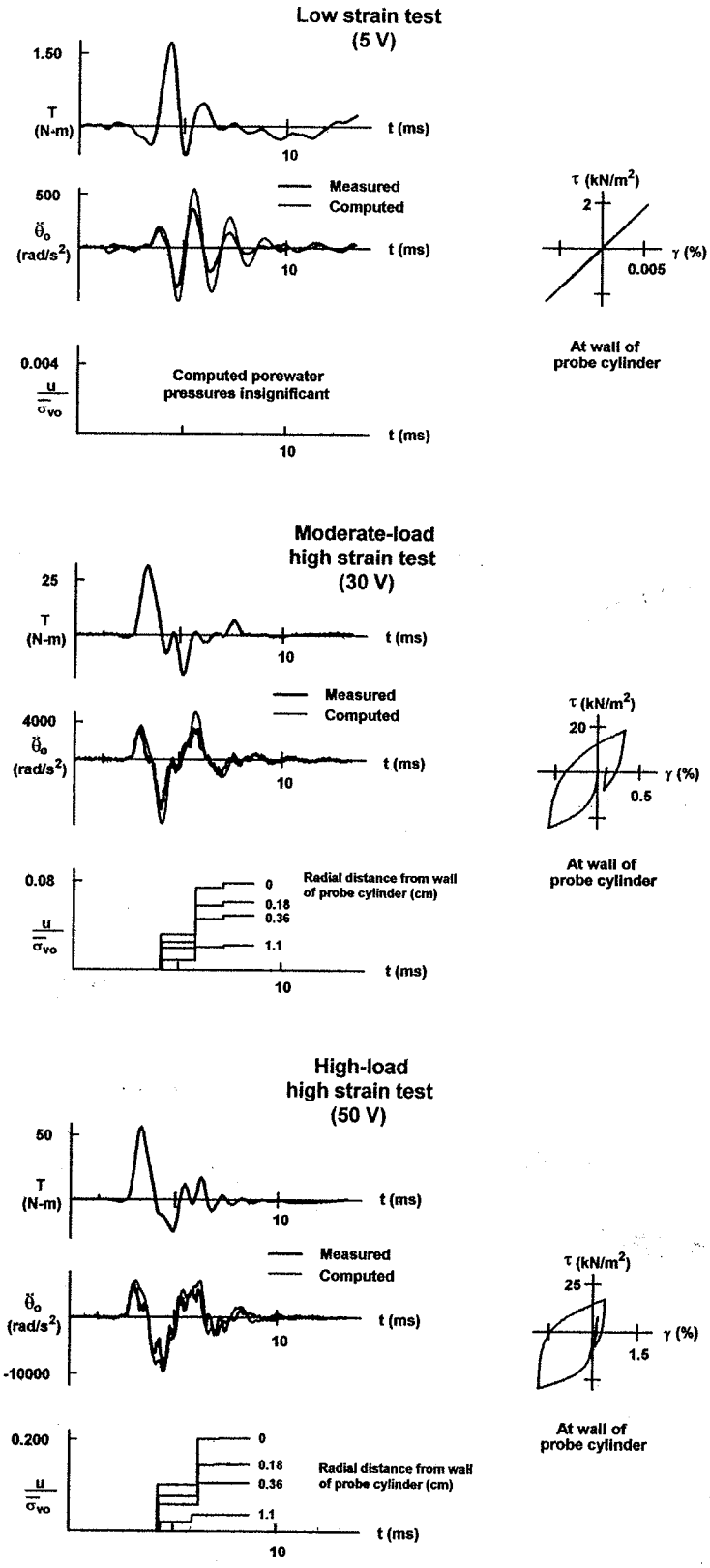

Figure 20: Results from representative impulse shear tests carried out within the upper layer of saturated silty sand at a depth of 5.18 m at the Treasure Island site (2002 testing program) and from the corresponding simulations using the values inferred for the parameters of the Ramberg-Osgood equations and with porewater pressure generation. A condition of liquefaction is considered to exist when $u/\bar{\sigma}_{vo} = 1$.

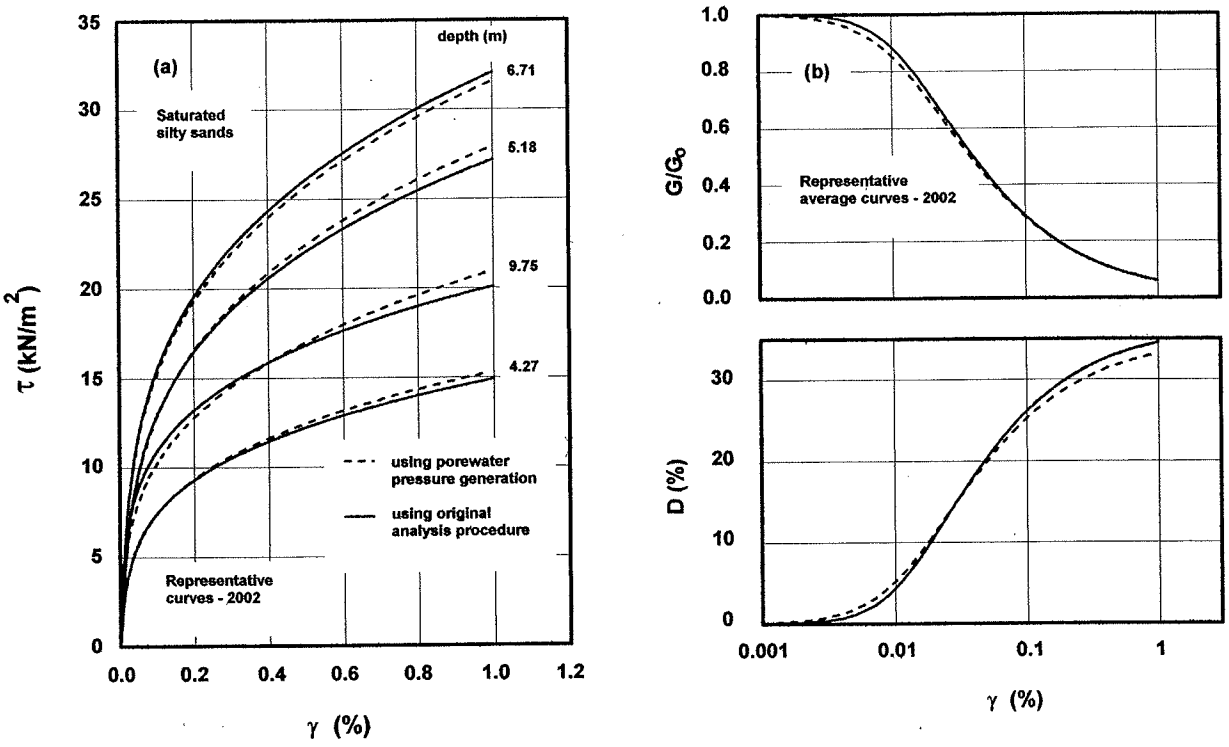

Figure 21: Idealized nonlinear inelastic shearing deformation characteristics inferred for the Treasure Island site from results of representative impulse shear tests conducted in the upper silty sand layer (2002 testing program).

probe cylinder; and the computed values of the porewater pressure ratio ($u/\bar{\sigma}_{vo}$) for selected radial distances from this wall.

The computed values for porewater pressures seem to be at least qualitatively reasonable. As would be expected with the limited numbers of cycles of loading, the pressures are of moderate levels. ($u/\bar{\sigma}_{vo}$ = 1 represents the state of liquefaction.) Also, the porewater pressures were computed to be greatest during the high-load high strain test and least during the low strain test and the levels of pressure generally drop with increasing radial distance from the wall of the probe cylinder.

The computed pressures did not have large effects on the inferred shearing deformation characteristics of the tested soils. In Fig. 21a, we show the shear stress vs strain curves we inferred using the porewater pressure generation model along with those inferred using our original analysis procedure. The former curves are nondegraded curves that are computed to exist prior to the development of any porewater pressures. The curves stemming from our original analysis procedure, in essence, include effects of porewater pressures, assuming they developed during the moderate-load high strain tests used to interpret test results. In this case, the curves are degraded curves that likely roughly represent averages of the characteristics existing during the tests. In Fig. 21b, we show representative average normalized secant shear modulus reduction and damping ratio curves for the nondegraded characteristics obtained using the porewater pressure generation model and the characteristics obtained using our original analysis procedure.

Though our simulations of impulse shear tests with porewater pressure generation are qualitatively reasonable, because of special issues that arise when using the porewater

pressure generation model to simulate such tests in particular and because of our very approximate approach in selecting values for the parameters of the model, there is uncertainty regarding quantitative precision. Using this added capability, we compute porewater pressures at the ends of half cycles of loading when shear stress vs strain curves reverse direction. Variations in porewater pressures between reversals that are not caused by the dissipation of porewater pressures are not described. (We have not yet modeled the dissipation of porewater pressures.) This practical simplification is believed to be satisfactory, in many cases, for the earthquake analysis procedures for which the model was developed (16); such procedures describe dynamic behavior over long durations (tens of seconds) and with many significant cycles of loading. However, impulse shear tests are of extremely short durations (~10 ms) and usually do not cause more than one significant cycle of loading. Observations of results of high strain laboratory cyclic tests conducted on samples of saturated sands show that porewater pressures can vary greatly during single cycles of significant loading (34). It would appear that with impulse shear tests involving at most one cycle of significant loading, the variations in porewater pressures during the cycle could possibly have sizable impacts on behavior. Additionally, since porewater pressures are computed only at reversals in loading, no pressures are computed to develop during the initial loading. Initial loading generally represents a substantial portion of high strain impulse shear tests. To be able to evaluate more fully any porewater pressure generation/dissipation modeling or to be more definitive with regards to porewater pressures developed when testing cohesionless soils it would be necessary to add to the impulse shear test the capability to measure porewater pressures.

High Strain Damping Ratios for Saturated Sandy Soils—The issue of high strain damping ratios for saturated sandy soils has been a source of uncertainty in the past. Our recent work provides insight on the issue. However, uncertainty still remains and broad and detailed study of the issue would be expected to be of value.

Our past work is discussed in detail in Ref. 17 (see App. A). For high strains we found that damping ratio curves inferred for the upper layer of soil at the Treasure Island site from results of impulse shear tests conducted as part of our 1996 testing program exceed both corresponding published general curves (curves compiled from many testing programs and representing large bodies of data) and published damping ratios inferred from specific results of laboratory tests carried out on samples from this layer. Of the many possible sources of the observed differences, to date, we have focused on two. One of these, applicable to the comparisons with general curves, is an apparent inconsistency: at higher strains, the general damping ratio curve we had used for sands fell roughly 25% below the curve that would be theoretically derived from the corresponding normalized secant shear modulus reduction curve. (When idealizing nonlinear inelastic shearing deformation characteristics assuming Masing's criterion [Ref. 27 as cited in Ref. 23], normalized secant shear modulus reduction curves, like shear stress vs strain curves, are primary functions. In contrast, damping ratio curves that represent hysteresis conventionally, as described, for example, in Ref. 17 (see App. A), are secondary functions that are fully derived from, and thus are fixed by, either one of the primary functions.) The second source of the observed differences on which we have focused, which applies to the comparison with the specific test results as well as to the comparisons with general damping ratio curves, was speculated to be buildups in porewater pressures during impulse shear tests.

Regarding our recent work, as shown by Fig. 17b, the high strain damping ratios inferred as part of our 2002 testing program show the same trends as those of our 1996 program. (We should note that, at lower strains, damping is underestimated when using the impulse shear test. This is because we do not yet represent low strain damping of the test soil in simulations of tests. Rather, to date, our priorities have been toward providing high strain information.) However, with respect to the comparison with the general damping ratio curve, if a damping ratio curve that

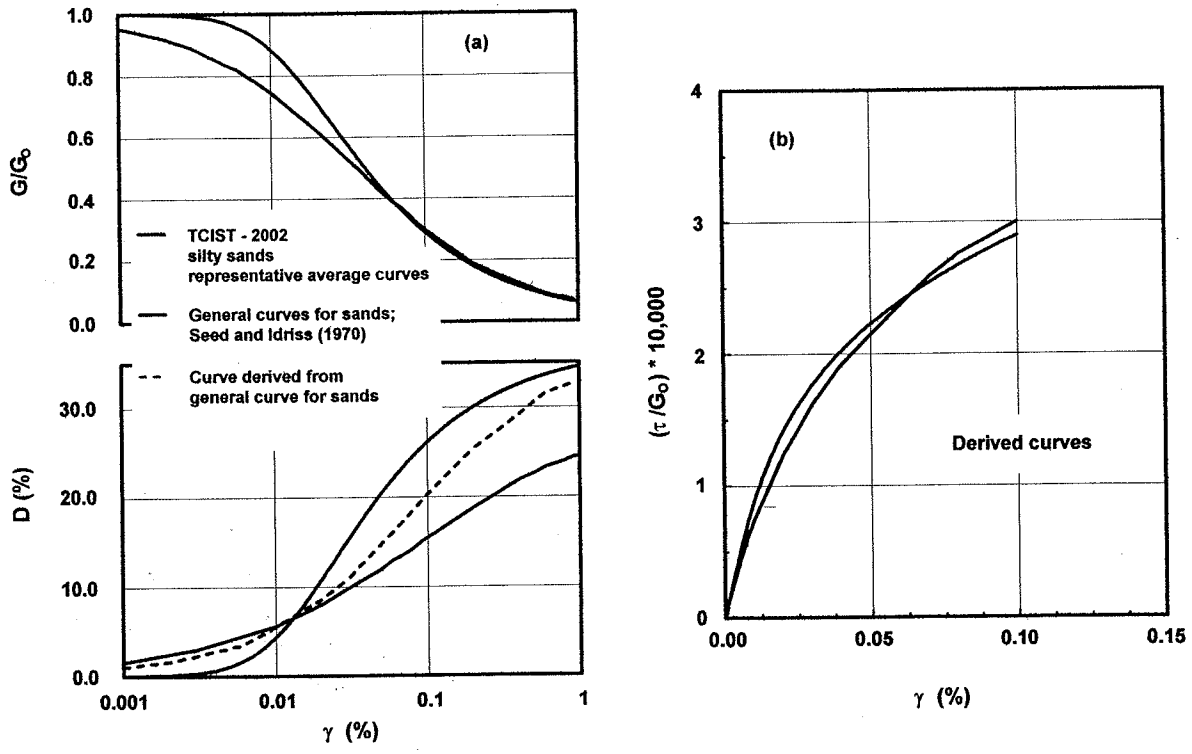

Figure 22: Comparisons between high strain information inferred from the results of representative impulse shear tests carried out in the upper silty sand layer at the Treasure Island site (2002 testing program) and published general curves for sands. (a) The general curves were scaled from Fig. 17b and the dashed damping ratio curve was derived from the general normalized secant shear modulus reduction curve by authors (17; see App. A) using conventional theory. (b) These shear stress vs strain curves were derived from the normalized secant shear modulus reduction curves shown in (a). The stresses are normalized by G_o/10,000 for convenience and the strains are limited because of inaccuracies in scaling at higher strains.

represents hysteresis assuming Masing's criterion is derived from the general normalized secant shear modulus reduction curve shown in Fig. 17b, as may be seen in Fig. 22a, the derived damping ratio curve differs from the general damping ratio curve and the damping ratio curve for the impulse shear test agrees more closely with the derived curve than with the general curve. These observations suggest that, on average, the shear stress vs strain curves of the soil samples on which the general curves are based did not precisely show idealized hysteresis that follows Masing's criterion and that this ideal better describes the characteristics of the sands tested by the impulse shear test than do the characteristics of those samples.

With respect to the comparison in Fig. 17b with the specific test results, though the agreement is within reason for high strain damping ratios (further discussed in following paragraph), uncertainty exists. Among other things, published results for sandy soils are somewhat at odds with each other. For example, in Fig. 23, we show results from the impulse shear tests we conducted in the silty sands of the Treasure Island site during 2002 superimposed on results of laboratory tests carried out on samples of soils, including sands, taken from the Lotung experimentation site in Taiwan. The upper 10 m of soil at this site seem quite similar, from standpoints of soil types, SPT measurements, and shear wave velocities (5) (12), to those at the Treasure Island site. However, our comparisons for the two sites differ. The results from the

Lotung site show the same trends in high strain damping ratios as the results from the impulse shear tests. Other published results (Fig. 20 of Ref. 41 and Fig. 6 of Ref. 36) also show consistently high values of damping ratio for sandy soils (exceeding the mean general curve shown in Fig. 17b) at high strain levels.

At this time, we do not know the specific reasons for the differences seen among the high strain damping ratios from various testing programs. However, it is important to note that it appears as if high strain damping ratio is a sensitive parameter for which it is quite difficult to establish values with meaningful precision. In Fig. 22b, we show normalized shear stress vs strain curves derived from the two normalized secant shear modulus reduction curves shown in Fig. 22a. In practical terms, there is very little difference between the two stress vs strain curves (3.5% difference at 0.1% strain, for example). Yet, the corresponding theoretically derived damping ratio curves, shown in Fig. 22a (maroon and dashed curves), show fair differences (23.6% difference at 0.1% strain, for example). Figure 17a implies that shear stress vs strain curves are extraordinarily sensitive to test conditions and the preceding observations suggest that this sensitivity would be magnified in damping ratio curves. Thus, it would seem to follow that even minor disturbances that would be hard to avoid could impact the ability to establish meaningful values of high strain damping ratios. This difficulty, we feel, may be reflected in the relative scatter seen in values of high strain damping ratio presented in the literature. For instance, within the strain range of 0.001 % to 0.1 %, the upper bound general damping ratio curve for sands shown in Fig. 17b is greater than the lower bound curve by factors ranging roughly from 2 to 4. In contrast, the factors for the corresponding normalized secant shear modulus reduction curves range from 1.1 to 1.7.

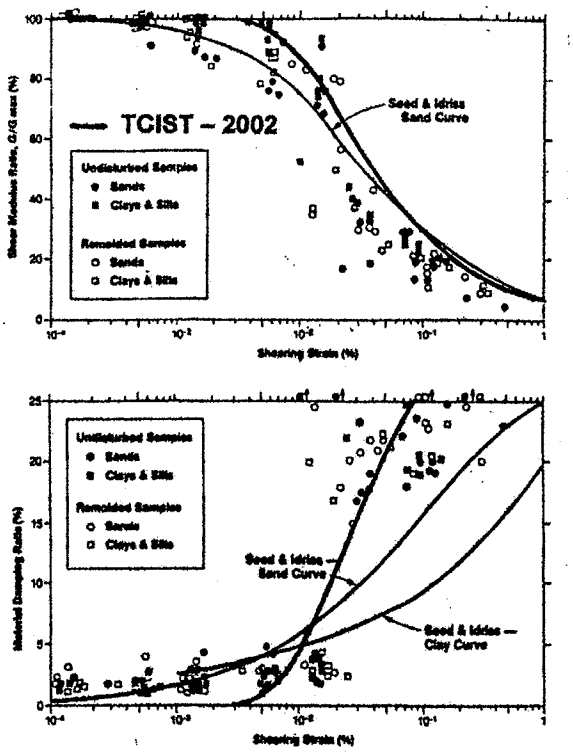

Figure 23: High strain information inferred from results of representative impulse shear tests conducted in the upper silty sand layer at the Treasure Island site (representative average curves) superimposed on corresponding information published in Ref. 38 and based on laboratory resonant column and cyclic triaxial tests conducted on samples of soil recovered from the Lotung experimentation site in Taiwan.

Lastly, with respect to the possibility that any porewater pressures that may have developed in the tested soils during impulse shear tests may have contributed to elevated high strain damping ratios, our simulations of impulse shear tests using the porewater pressure generation model tend to support this possibility. The analysis results presented in Fig. 21b indicate that, at higher levels of shear strain, the nondegraded damping ratio curve obtained using the porewater pressure generation model falls below the curve inferred using our original analysis procedure. To be able to establish more fully any relations that may exist between high strain damping ratios of sandy soils and buildups in porewater pressures it would be necessary to add to the impulse shear test the capability to measure porewater pressures.

Estimating In Situ Resistances to Liquefaction and Related Deformations—With the 2002 testing program at the Treasure Island site, the impulse shear test continues to show promise toward being able to provide reasonably precise indications of in situ resistances to liquefaction and related deformations. As background to our 2002 work, we summarize the two sets of observations that brought this potential capability to light.

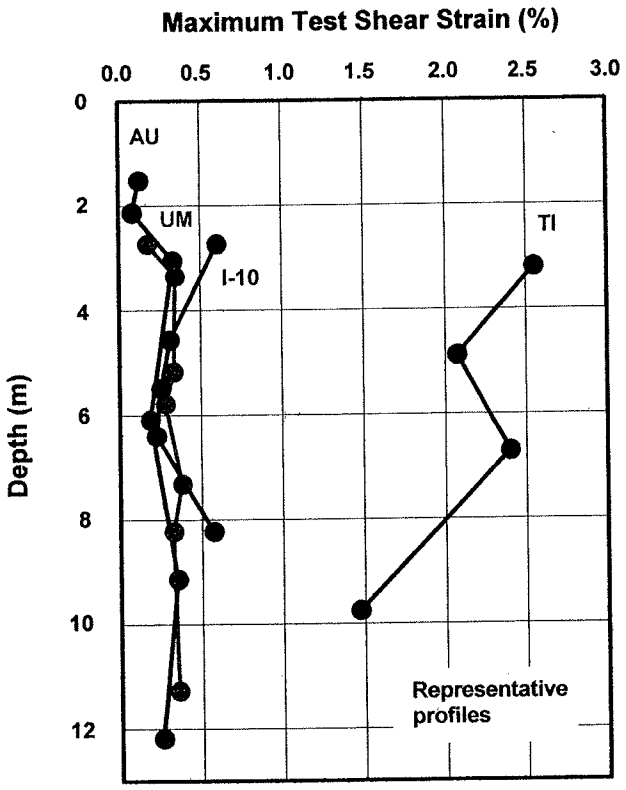

Figure 24: Profiles of maximum test shear strains for impulse shear tests conducted at four sites (AU, I-10, TI, and UM).

First, maximum test shear strains (defined on p. 2) have been found to be far larger in highly liquefiable soils than in soils that are likely resistant to liquefaction. In Fig. 24, we show profiles of the maximum test shear strains for four sites at which we have conducted impulse shear tests (9) (17; see App. A). (These are sites for which at least low strain information was available for comparison purposes.) The strains for the Treasure Island site (TI), at which we tested highly liquefiable soils (1996 testing program), are consistently larger than those for the other sites, which, except possibly for the soil at a depth of 8.23 m at the I-10/La Cienega Blvd. (I-10) site, are believed to be highly resistant to liquefaction.

The second set of observations (19) that suggests that the impulse shear test may have the potential for providing reasonably precise indications of in situ resistances of soils to liquefaction is the significant and logical differences among information inferred from the results of impulse shear tests conducted in saturated silty sands that, apparently, were loose (likely, highly liquefiable and deformable), medium-dense (likely, moderately liquefiable and deformable), and dense (likely, highly resistant to liquefaction and deformations). The tests were carried out at a highway bridge construction site along Bayou Chico in Pensacola, Florida (7). The test depths (roughly 7.5 - 8.5 m) and thus the confining pressures for the tested soils were roughly equal. Therefore, confining pressure may reasonably be ruled out as a major factor in differences among test results.

With respect to differences among results, first, the maximum force needed to penetrate the cylinder of the probe into the tested soil was greatest for the dense sand (~28 kN), of an intermediate level for the medium-dense sand (~22 kN), and least for the loose sand (~8 kN). Second, the low strain shear modulus inferred for the dense sand (77.2 MN/m^2) was much greater than that inferred for the loose sand (27.1 MN/m^2), and that for the medium-dense sand (60.2 MN/m^2) fell in between. Third, the results of the high strain impulse shear tests conducted in the three sands were considerably different from each other. For example, in Fig. 25 we show test and analysis results for moderate-load high strain tests (30 V) conducted in the three soils. For each test, are shown the measured applied torque; the angular accelerations of the instrumented head that were measured and that were computed as part of the corresponding most representative simulation; and shear stress vs strain curves described by this simulation for the test soil at the wall of the cylinder of the probe. Various differences may be seen: the

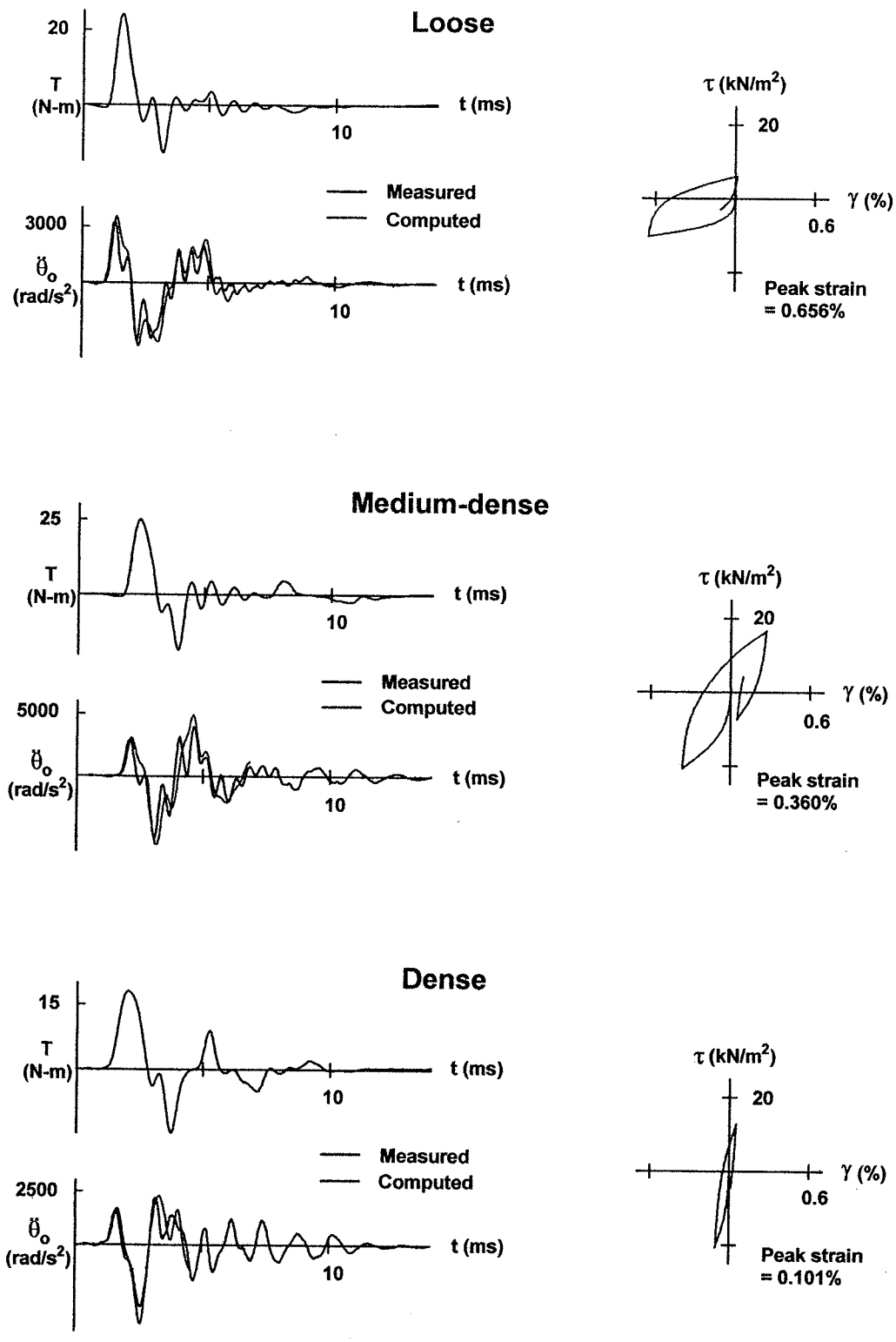

Figure 25: Results from moderate-load high strain (30 V) impulse shear tests conducted in saturated silty sands along Bayou Chico in Pensacola, Florida (7) and from the corresponding most representative analytical simulations. Note that the stress vs strain curves are all of the same scale. Also, the short durations of the computed angular accelerations reflect superseded practices (see Interpretations of Test Results, p. 8).

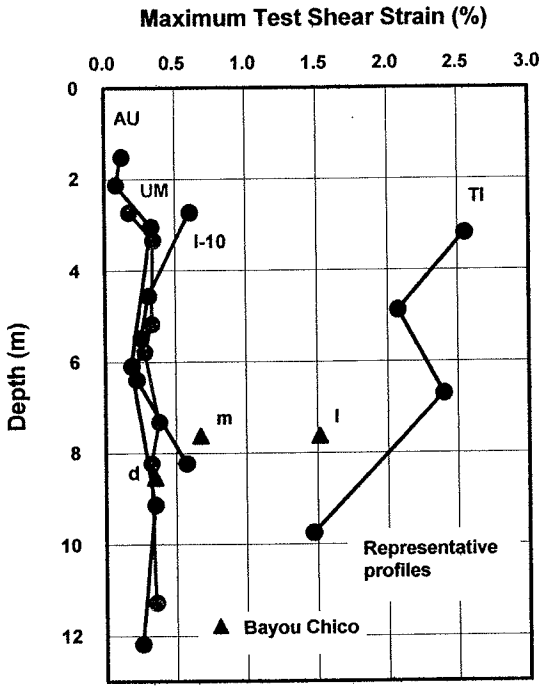

Figure 26: Maximum test shear strains for impulse shear tests conducted in saturated loose (l), medium-dense (m), and dense (d) silty sands at the Bayou Chico site in Pensacola, Florida (7) superimposed on profiles of maximum test shear strains shown in Fig. 24.

dominant frequency of the angular acceleration of the instrumented head was greatest for the dense sand and least for the loose sand; the decay of this angular acceleration was most pronounced for the loose sand and least pronounced for the dense sand; and the computed peak shear strain was greatest for the loose sand (0.66%), least for the dense sand (0.10%), and of an intermediate level for the medium-dense sand (0.36%). Fourth, in Fig. 26, we show the maximum test shear strains (defined on p. 2) for the three sands superimposed on the profiles of the maximum test shear strains presented earlier in Fig. 24. The strain for the dense sand plots along with the likely liquefaction resistant soils (I-10, UM, and AU), the strain for the loose sand plots along with the highly liquefiable soils (TI), and the strain for the medium-dense sand plots in between the two. On the basis of these findings, we would expect highly liquefiable cohesionless soils to show low penetration resistances and low strain shear moduli, and high maximum test shear strains (large deformations); dilating cohesionless soils that are resistant to liquefaction to show high penetration resistances and low strain shear moduli, and low maximum test shear strains (limited deformations); and moderately liquefiable cohesionless soils to show intermediate penetration resistances, low strain shear moduli, and maximum test shear strains.

The results from our 2002 Treasure Island testing program are consistent with these two sets of observations. The loose sandy layer, which is likely highly liquefiable, showed markedly different characteristics and behaviors than the clay layer, which, presumably being highly resistant to liquefaction, serves as a useful reference. Herein, we discuss two soil characteristics parameters and one behavior parameter that show potential for indicating resistances to liquefaction. These are the low strain shear modulus; the secant shear modulus for a specified moderate shear strain; and the maximum test shear strain.

The low strain shear modulus profile we inferred for the Treasure Island site is presented in Fig. 10. On the basis of, among other things, the past work we presented above for the Bayou Chico site, we judge the low strain shear moduli for the silty sand layer to be of moderate levels that indicate the relative densities of the layer to range roughly from loose to the loose side of medium-dense (highly liquefiable). This is consistent with results from SPTs conducted at the Treasure Island site (5). In our work for the Bayou Chico site, as brought out above, we found low strain shear moduli obtained using the impulse shear test to be sensitive to the apparent relative density and thus, the liquefiability of saturated silty sands. However, from Fig. 10, it does not appear that this ability of the low strain shear modulus to indicate liquefaction resistance of cohesionless soils extends to soils having cohesive components. The shear moduli in the figure do not reflect the apparent relative liquefiability of the sandy soils and the clay. That is, the highly liquefiable sandy layer generally shows greater shear moduli than the

liquefaction resistant clay layer. Nor is there any indication that the sand/clay transition sublayer, which apparently contains clay, is any more resistant to liquefaction than the silty sands above.

In contrast, perhaps because it is a high strain parameter, the secant shear modulus for a moderately high strain of, for example, 0.5% seems to relate to liquefaction resistance in a broad manner. The profile we inferred for this high strain shearing rigidity parameter is shown in Fig. 27. The clay layer shows greater values for the parameter than the silty sand layer and the sand/clay transition sublayer shows an intermediate value. The ability to indicate, reasonably precisely, resistances to liquefaction over a broad range of soil types would be expected to be of practical value, in particular, in critical and difficult borderline cases involving mixed soils.

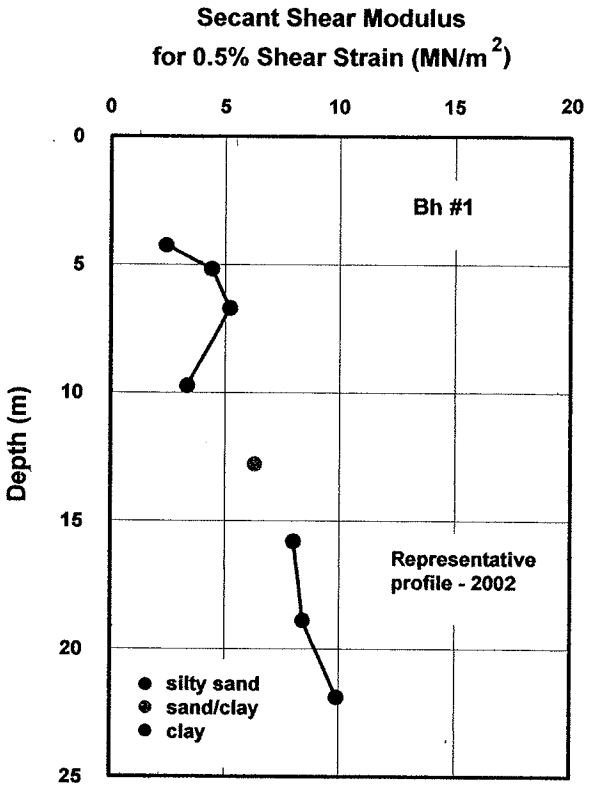

Figure 27: Profile of the secant shear modulus for a shear strain of 0.5% inferred for the Treasure Island site from results of representative impulse shear tests (2002 testing program).

Profiles of the maximum test shear strains we inferred are shown in Fig. 28. Both peak and peak to peak strains are plotted. The values of these parameters also appear to reflect the liquefiability of the tested soils. That is, the highly liquefiable soils show high values for these parameters whereas the soils that are likely resistant to liquefaction show low values. However, the peak maximum test shear strain is more sensitive to liquefaction resistance than the peak to peak maximum test shear strain. The reason for this lies in effects of soil type on the development of shear strains within the tested soils along the wall of the probe cylinder during high-load high strain impulse shear tests. As shown in Fig. 29a, typically, in the saturated loose sandy soils these strains damped out fairly rapidly after the first peak, which was usually the peak maximum test shear strain. As a result, for such soils, peak to peak strains differ very little if any from the peak strains. In contrast, as shown in Fig. 29b, the strains normally did not damp out as rapidly in the clay soils. Thus, the peak to peak strains for the clay soils are very much larger than the peak strains. In turn, the differences between the peak to peak maximum test shear strains of the silty sands and of the clays are not as great as the differences between the peak maximum test shear strains for these soils. We should note that the values of these behavior parameters are affected by dynamics; therefore, the parameters are not pure measures of soil characteristics.

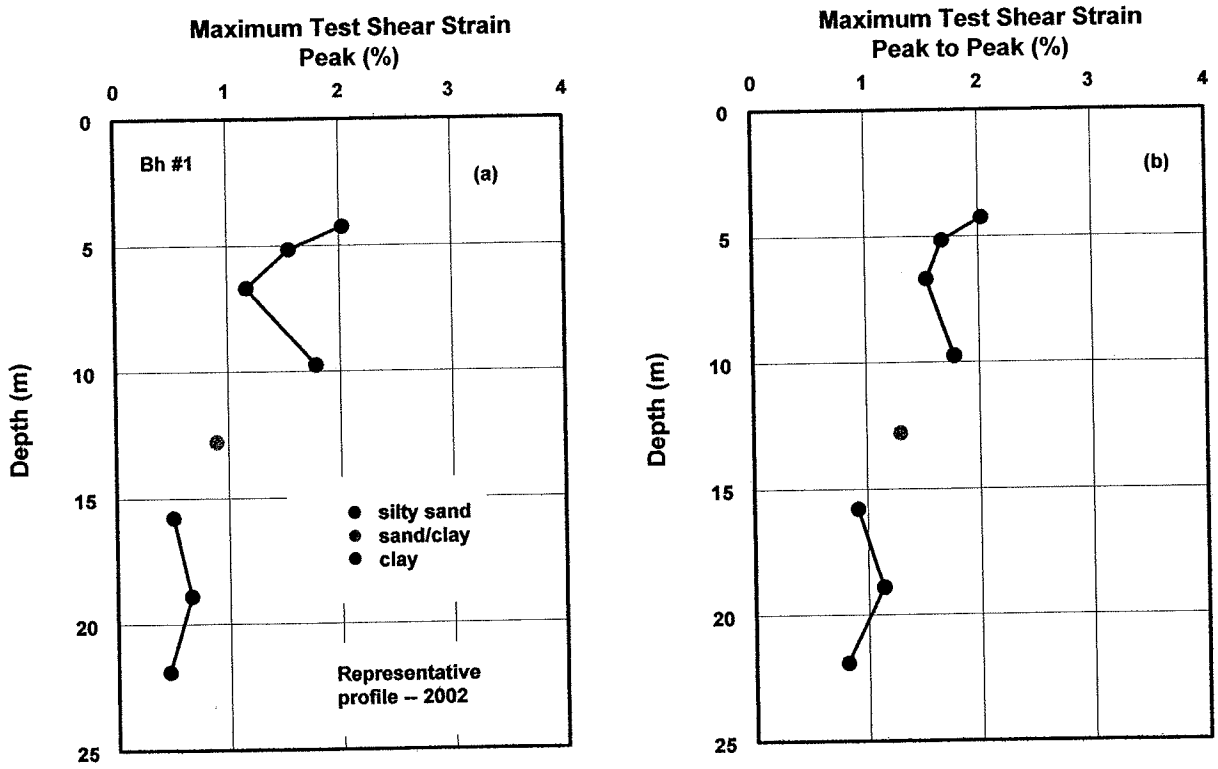

Figure 28: Profiles of the maximum test shear strains inferred for the Treasure Island site from results of representative impulse shear tests (2002 testing program).

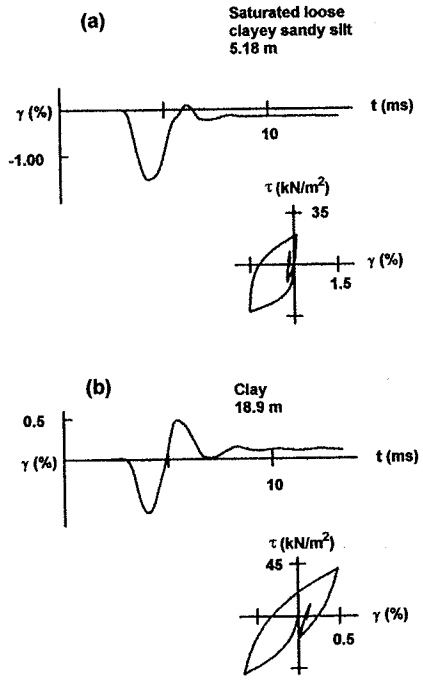

Figure 29: Typical computed behaviors of tested soils at the wall of the probe cylinder during high-load high strain (50 V) impulse shear tests conducted at the Treasure Island site (2002 testing program).

Conclusions

Our work and experiences during the subject project suggest that the impulse shear test

1) is a viable means for providing, for soils that are highly relevant to earthquake engineering, detailed information on in situ nonlinear inelastic shearing deformation characteristics needed for geotechnical earthquake engineering analysis procedures;
2) is a promising technology for providing reasonably precise indications of in situ resistances of soils to liquefaction and related deformations; and
3) will be highly usable, efficient, reliable, robust, and economical when adapted for production use.

Near-Term Future Work

The continued promise shown by the impulse shear test suggests that further effort should be placed toward the development of the test and toward bringing this technology to practice effectively. Near-term work that would logically follow the subject project includes

1) developing and manufacturing a highly usable, efficient, reliable, robust, and economical field prototype production impulse shear testing system;
2) adding to the impulse shear test the capability to measure porewater pressures; and
3) continuing the definitive field verification of the impulse shear test initiated by the project.

The first and third of these would be expected to attract greater interest in the use of the impulse shear test in practice. The second would be expected to help toward addressing relevant issues in the testing of saturated cohesionless soils with greater certainty than has previously been the case.

References

1. Anderson, D.G. and Espana, C., "Evaluation of In Situ Testing Methods for High-Amplitude Dynamic Property Determination," rep. by Fugro, Inc., Long Beach, Calif., EPRI NP-920, Nov. 1978.
2. Bielak, J. and Romo, M., "Working Group Conclusions on Geotechnical Engineering and Foundations," Lessons Learned from the 1985 Mexico Earthquake, EERI, Dec. 1989.
3. Briaud, J.-L., R.L. Lytton, and J.-T. Hung, "Obtaining Moduli from Cyclic Pressuremeter Tests," *J. Geotech. Eng.*, ASCE, 109(5), 1983.
4. Committee on Earthquake Engineering, Commission on Engineering and Technical Systems, and the National Research Council, "Liquefaction of Soils During Earthquakes," rep. for NSF, Nat. Acad. Press, Wash., D.C., 1985.
5. de Alba, P., J. Benoit, T.L. Youd, A.F. Shakal, D.G. Pass, and J.J. Carter, "Deep Instrumentation Array at Treasure Island Naval Station, NEHRP report to Congress, the October 17, 1989, Loma Prieta, California, Earthquake," *US Geol. Survey,* in press in 1993.
6. de Alba, P. and J.R. Faris, "Workshop on Future Research Deep Instrumentation Array Treasure Island NGES," Treasure Island, San Francisco Bay, July 27, 1996.

7. Dynamic In Situ Geotechnical Testing, Inc., "In Situ Low and High Strain Deformation Characteristics for Shallow Layers of Soil: Bayou Chico Site, Pensacola, Florida and Auburn University Site, Spring Villa, Alabama," rep., Baltimore, Md., Apr. 1998. (Available from firm, 410-415-5903.)
8. Dynamic In Situ Geotechnical Testing, Inc., "In Situ Nonlinear Shear Stress vs Strain Characteristics for Shallow Layers of Soil: I-10/La Cienega Blvd. Undercrossing, Los Angeles, California," rep., Baltimore, Md., Nov. 1996. (Available from firm, 410-415-5903.)
9. Dynamic In Situ Geotechnical Testing, Inc., "Initiation of Definitive Field Verification of Torsional Cylindrical Impulse Shear Test Phase I," draft rep., Baltimore, Md., Oct. 2002. (Available from firm, 410-415-5903).
10. EERI, "Loma Prieta Earthquake Reconnaissance Report," *Earthquake Spectra*, Supp. to Vol. 6, May 1990.
11. EERI, "The Hyogo-ken Nanbu Earthquake January 17, 1995 Preliminary Reconnaissance Report," Feb. 1995.
12. Elgamal, A. –W., M. Zeghal, H. T. Tang, and J. C. Stepp, "Lotung Downhole Array. I: Evaluation of Site Dynamic Properties," *J. of Geotech. Eng.,* ASCE, 121 (4), April 1995.
13. Faris, J.R., personal communication, Aug. 2002.
14. FHWA, National Geotechnical Experimentation Sites database. (Software available from FHWA. Contact M. Adams at FHWA, Turner-Fairbank Highway Research Center, McLean, Va., 703-285-2161.) 1995.
15. Finn, W. D. L., personal communication, approx. 1982.
16. Finn, W.D.L., Lee, K.W., and Martin, G.R., "An Effective Stress Model for Liquefaction," *J. of the Geotech. Eng. Div.,* ASCE, June 1977.
17. Henke, R. and Henke, W., "In Situ Nonlinear Inelastic Shearing Deformation Characteristics of Soil Deposits Inferred Using the Torsional Cylindrical Impulse Shear Test," *Bull. of Seism. Soc. of Am.,* June 2002. (Included in App. A.)
18. Henke, R. and W. Henke, Method and Apparatus for Testing Soil. U.S. patent no. 4,594,899. International patents also exist. 1986.
19. Henke, W. K. and R. Henke, "In situ impulse shear tests of loose and dense, saturated, silty sand," in *Earthquake Geotech. Eng.,* P. S. Sêco e Pinto (Ed.), Proc. of the Second Int. Conf. on Earthquake Geotech. Eng., Lisboa, Portugal, 21-25 June 1999.
20. Henke, W. and Henke, R., "Laboratory Evaluation of In Situ Geotechnical Torsional Cylindrical Impulse Shear Test for Earthquake Resistant Design," *Bull. of Seism. Soc. of Am.,* Feb. 1993.
21. Henke, W. and Henke, R., "Simplified In Situ Torsional Cylindrical Impulse Shear Test," *Earthquake Resistant Construction & Design,* S. Savidis (Ed.), Proc. of the 2nd Int. Conf. on Earthquake Resistant Construction and Design, Berlin, Germany, June 1994.
22. Hwang, S.K. and K.H. Stokoe, II, "Dynamic Properties of Undisturbed Soil Samples from Treasure Island, California," Geotech. eng. rep. GR93-4, Univ. of Texas, Austin, 1993.
23. Idriss, I.M., Dobry, R., and Singh, R.D., "Nonlinear Behavior of Soft Clays During Cyclic Loading," *J. of the Geotech. Eng. Div.*, ASCE, Dec. 1978.
24. Jamiolkowski, M., Lo Presti, D.C.F., and Pallara, O., "Role of In Situ Testing in Geotechnical Earthquake Engineering," preprint of state-of-the-art paper, Proc., 3rd Int. Conf. on Recent Advances in Geotech. Earthquake Eng. and Soil Dynamics, St. Louis, Mo., Apr. 1995.

25. Lee, M.K.W., and Finn, W.D.L., DESRA-2C, manual for computer program DESRA, Univ. of British Columbia, revised, 1991.

26. Martin, G.R., Finn, W.D.L., and Seed, H.B., "Fundamentals of Liquefaction under Cyclic Loading," *J. of the Geotech. Eng. Div.*, ASCE, May 1975.

27. Masing, G., "Eigenspannungen und Verfestigung beim Messing," *Proc. of the Second Int. Congress of Applied Mechanics*, Zurich, 1926.

28. National Institute of Standards and Technology, "Performance of Structures During the Loma Prieta Earthquake of October 17, 1989," Spec. Pub. 778, Jan. 1990.

29. "Proceedings: NSF/EPRI Workshop on Dynamic Soil Properties and Site Characterization," EPRI NP-7337, Palo Alto, Calif., June 1991.

30. Richart, F.E., Jr. and Wylie, E.B., "Influence of Dynamic Soil Properties on Response of Soil Masses," Symp. on Structural and Geotech. Mech., Univ. of Illinois, Urbana, Oct. 1975.

31. Roblee, C.J. and M.F. Riemer, "The Downhole Freestanding Shear Device Concept," in *Geotech. Earthquake Eng. and Soil Dynamics III*, ASCE, held in Seattle, Washington, August 3-6, 1998.

32. Roblee, C.J., Li, X.S., Chan, C.K., Idriss, I.M., Wang, G., Herrmann, L.R., and Jackura, K.A., "Feasibility of a Tool for In Situ Measurement of Material Properties of Clays Over a Wide Strain Range," *Dynamic Geotech. Testing: Second Vol., ASTM STP 1213,* R.J. Ebelhar, V.P. Drnevich, and B.L. Kutter (Eds.), ASTM, 1994.

33. Salgado, R., Drnevich, V.P., Ashmawy, A., Grant, W.P., and Vallenas, P., "Interpretation of Large-Strain Seismic Cross-Hole Tests", *J. of Geotech. and Geoenvironmental Eng.*, ASCE, Apr. 1997.

34. Seed, H.B., "Evaluation of Soil Liquefaction Effects on Level Ground During Earthquakes," *Liquefaction Problems in Geotech. Eng.,* Preprint 2752, ASCE Conv., Philadelphia, Pa., Sept./Oct. 1976.

35. Seed, H.B. and I.M. Idriss, "Soil Moduli and Damping Factors for Dynamic Response Analyses," rep. no. EERC 70-10, Earthquake Engineering Research Center, Univ. of California, Berkeley, 1970.

36. Seed, H. B., R. T. Wong, I. M. Idriss, and K. Tokimatsu, "Moduli and Damping Factors for Dynamic Analyses of Cohesionless Soils," *J. of Geotech. Eng.,* ASCE, Nov. 1986.

37. Stone, W.C., Yokel, F.Y., Celebi, M., Hanks, T., and Leyendecker, E.V., "Engineering Aspects of the September 19, 1985 Mexico Earthquake," NBS (now NIST) Building Science Series 165, May 1987.

38. Tang, H.T., J.C. Stepp, and Y.K. Tang, "Strong Motion Array Data – Applications for Blind Predictions and Nuclear Power Plant Seismic Response Studies," *Geotech. News*, 9(1), 1991.

39. Vucetic, M. and Dobry, R., "Effect of Soil Plasticity on Cyclic Response," *J. Geotech. Eng.,* ASCE, Jan. 1991.

40. Woods, R.D., "Field and Laboratory Determination of Soil Properties at Low and High Strains," Proc., 2nd Int. Conf. on Recent Advances in Geotech. Earthquake Eng. and Soil Dynamics, St. Louis, Mo., Mar. 1991.

41. Zeghal, M., A. –W. Elgamal, H. T. Tang, and J. C. Stepp, "Lotung Downhole Array. II: Evaluation of Soil Nonlinear Properties," *J. of Geotech. Eng.,* ASCE, April 1995.

Appendix A: 2002 *BSSA* Article

This appendix consists of a 2002 *BSSA* journal article by our firm that summarizes preliminary field impulse shear tests of the prototype impulse shear testing system that we designed and constructed for FHWA. These represent our first field impulse shear tests.

Bulletin of the Seismological Society of America, Vol. 92, No. 5, pp. 1970–1983, June 2002

In Situ Nonlinear Inelastic Shearing Deformation Characteristics of Soil Deposits Inferred Using the Torsional Cylindrical Impulse Shear Test

by Robert Henke and Wanda K. Henke

Abstract This article summarizes preliminary field evaluations of a new in situ geotechnical test, the torsional cylindrical impulse shear test. The impulse shear test provides, for soil deposits, detailed information on in situ nonlinear inelastic shearing deformation characteristics needed for dynamic geotechnical earthquake analysis procedures. The test addresses the issue of obtaining such information in a practical manner without disturbing the tested soils excessively. Herein, we present soil characteristics inferred from results of impulse shear tests conducted at four sites using a field prototype testing system. One of the sites is the I-10/La Cienega Blvd. undercrossing in Los Angeles, where a freeway structure collapsed during the 1994 Northridge earthquake, and another is the National Geotechnical Experimentation Site on Treasure Island in the San Francisco Bay. The four sites cover a broad range of soil conditions relevant to earthquake engineering. These include soft to medium-stiff clays and saturated loose sands. Comparisons between our results and published information suggest that the impulse shear test is a promising means for obtaining in situ nonlinear inelastic shearing deformation characteristics of soil deposits.

Introduction

This article summarizes preliminary field evaluations of a new in situ geotechnical test, the torsional cylindrical impulse shear test (Henke and Henke, 1986, 1993b). The impulse shear test provides, for soil deposits, detailed information on in situ nonlinear inelastic shearing deformation characteristics needed for dynamic geotechnical earthquake analysis procedures. Such procedures are used to predict the behaviors of soil deposits (motions and occurrences of liquefaction) during earthquakes. The information provided includes idealized nonlinear inelastic shear stress versus strain curves (τ versus γ), including low-strain shear moduli (G_o) and their alternative representations, secant shear modulus reduction curves (G versus γ). Equivalent viscous damping ratio curves (D versus γ) may be derived from the former. We present soil characteristics inferred from results of impulse shear tests conducted at four sites. These evaluative tests were conducted using a field prototype testing system constructed for the U.S. Federal Highway Administration. This article is a sequel to a report on the laboratory evaluation of a laboratory prototype impulse shear testing system (Henke and Henke, 1993b). For brevity, we minimize repetition from that article. Further details regarding the material provided herein are reported by Dynamic In Situ Geotechnical Testing, Inc. (2000).

Symbols and Abbreviations

The following are abbreviations, variables, and symbols used in this article: AU, Auburn University site; D, equivalent viscous damping ratio; FHWA, U.S. Federal Highway Administration; G, secant shear modulus; G_{max} or G_o low-strain shear modulus; I-10, I-10/La Cienega Blvd. site; NSF, National Science Foundation; PI, plasticity index; R, parameter of Ramberg–Osgood equations; Rosrine, resolution of site response issues from the Northridge earthquake; T, applied torque; t, time; TCIST, torsional cylindrical impulse shear test; TI, Treasure Island site; UM, University of Massachusetts site; α, parameter of Ramberg–Osgood equations; γ, shear strain; θ, angular displacement of instrumented head about longitudinal axis of probe; θ_i, angular displacement of ith mass about longitudinal axis of model of probe; τ, shear stress; τ_{ref}, parameter of Ramberg–Osgood equations; and τ_y, parameter of Ramberg–Osgood equations.

Background Summary

Problem Addressed

The impulse shear test addresses the persistent problem of obtaining the information of interest on soil characteristics in a practical manner without disturbing in situ conditions excessively. Disturbances can create considerable uncertainty in predictions of behaviors of soil deposits during earthquakes. This can lead to unconservative or to costly, overly conservative designs for constructed facilities located in seismically active areas.

Comparable Technologies

Various geotechnical testing technologies are available for estimating the soil characteristics of interest (Henke and Henke, 1993b). Those most comparable to the impulse shear test are a method centered on a "downhole freestanding shear device" (Roblee and Riemer, 1998); a "large-strain seismic crosshole test" (Salgado *et al.*, 1997); and the pressuremeter test (Briaud *et al.*, 1983). The first method applies to clayey soils. Basically, a cylindrical sample is carved in the soil below the base of a borehole and a strain-gauged membrane is placed over the sample. The sample is first subjected to a confining pressure and then to a torsional shear loading. Applied torque and membrane strain are measured. Using the second method, a high-strain impulsive shearing disturbance is introduced into a soil deposit. Wave and particle velocities are measured using motion sensors lodged in boreholes. With the pressuremeter test, a tubular member with a concentric membrane is inserted into a soil deposit. Pressure is applied to the membrane, which expands laterally into the surrounding soil. The applied pressure and deformation of the membrane are measured. In situ nonlinear inelastic shearing deformation characteristics may be inferred from the measurements made in each of these testing methods.

Basic Idea of Impulse Shear Test

Figure 1a shows the basic idea of the field impulse shear test. A single open-ended cylinder (diam. ~7 cm) attached to a wireline probe is penetrated carefully into the soil below the base of a borehole. (The borehole is drilled using a conventional hollow-stem auger assembly that is plugged during drilling.) The test soil surrounds the lower portion of the cylinder. In a single test, an impulsive torque of a selected level is applied to the cylinder through an instrumented head. In response, torsional shear waves propagate through the test soil and the instrumented head–cylinder assembly rotates dynamically in a manner that is strongly dependent on the shearing deformation characteristics of the test soil. These characteristics are inferred from torque and angular acceleration measurements (made at the instrumented head) by simulating tests analytically. In combination, the basic configuration and elements of the test, the global measurements (nonstress and nonstrain) made, and the use of a fairly descriptive but practical analytical procedure to link these measurements to soil shear stresses and strains are intended to result in an effective balance between precision and simplicity.

Steps toward Reducing Disturbances

Regarding equipment, the cylinder of the probe, shown in Figures 1b and 2, includes several features to reduce disturbances to the test soil. The cylinder is precisely machined and its penetrating edge is beveled to minimize disturbances during penetration. The outer, active surface of the cylinder is grooved longitudinally to reduce slip during testing. To ensure that tests are conducted on deeper, less disturbed soil, the upper portion of the cylinder is machined smooth to a radius somewhat less than that of the roots of the grooves and is polished to provide an inactive surface that does not grip the soil. To minimize the influence of the soil within the cylinder on its motion (the soil inside the cylinder is not tested), the inner surface is machined smooth and polished, soil is diverted away from the surface by a jutted penetrating edge, and confining pressure on the soil within the cylinder

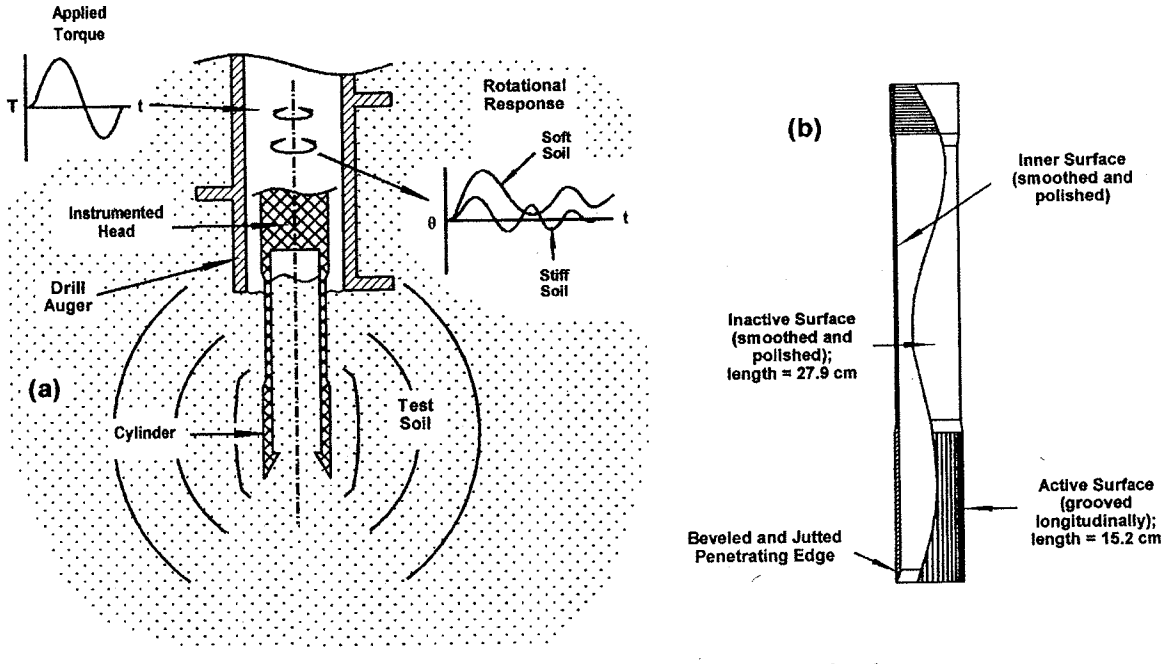

Figure 1. Field impulse shear test: (a) basic idea; (b) cylinder of probe.

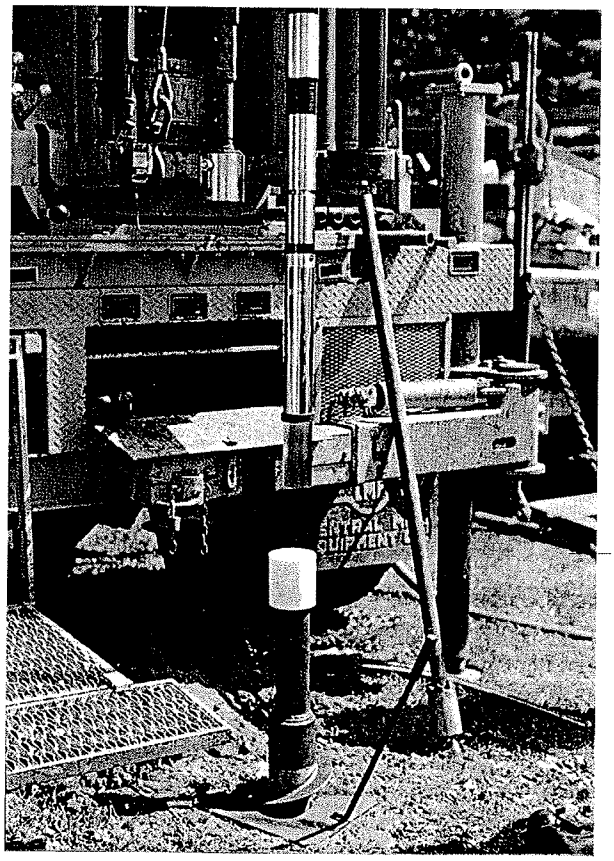

Figure 2. Cylinder of probe prior to testing.

is minimized by providing excess volume (through added length).

In preparing for tests, a relatively narrow auger is used to reduce the depth to which the disturbed zone directly below the base of the borehole extends. We also fill the auger assembly with drilling fluid. This lubricates the smooth, polished surfaces of the probe cylinder and reduces the possibility of developing unfavorable pressure gradients in the pore fluid below the base of the borehole. Such gradients can disturb the test soil. Lastly, the penetration of the probe cylinder into the test soil is carried out in a carefully controlled manner.

In testing at a given depth, low-strain tests, conducted using low levels of loading, are carried out first. These result in estimates of linear deformation characteristics. Then, a series of high-strain (herein, roughly greater than $\gamma = 0.001\%$) tests is conducted using increasingly higher levels of loading. These lead to estimates of nonlinear inelastic deformation characteristics.

Interpreting Test Results

To interpret results from an impulse shear test, an analytical model (Henke and Henke, 1993a) of a test is constructed. Figure 3 shows such a model. The measured torque is applied to the model. The computed and measured angular

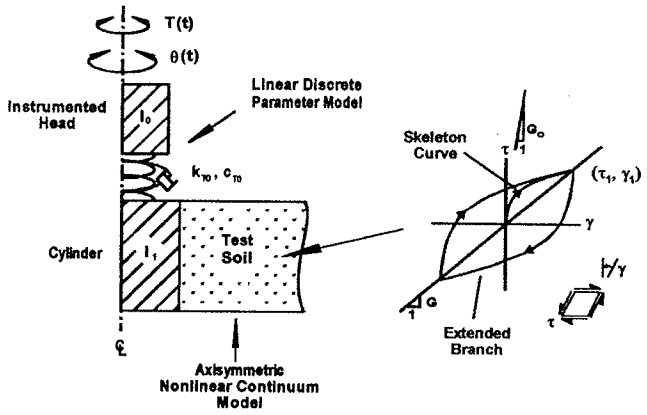

Figure 3. Analytical model of impulse shear test. I_i is the mass moment of inertia of the ith mass, k_{To} is torsional stiffness, and c_{To} is the torsional damping coefficient, each about the longitudinal centerline.

accelerations of the instrumented head are compared. The soil characteristics of interest are varied in search of the closest agreement between the two (most representative simulation). The corresponding soil characteristics are considered representative of those of the test soil. Two new elements of this procedure are discussed. These are revisions to the Ramberg–Osgood equations and to the procedure we use to establish most representative simulations. We currently use the Ramberg–Osgood equations to describe soil deformation characteristics in our simulations of impulse shear tests and in reporting interpretations of test results.

The Ramberg–Osgood equations are discussed in detail by Idriss *et al.* (1978) and Richart and Wylie (1977). These equations may be used to represent (1) either nonlinear inelastic shear stress versus strain curves or, the equivalent, secant (or tangent) shear modulus versus shear strain curves and (2) equivalent viscous damping ratio versus shear strain curves, often presented along with the latter.

The Ramberg–Osgood equation that may be used to describe idealized skeleton shear stress versus strain curves such as that shown in Figure 3 is given by Richart and Wylie (1977) as

$$\gamma = \frac{\tau}{G_o}\left[1 + \alpha\left|\frac{\tau}{\tau_y}\right|^{R-1}\right]. \qquad (1)$$

The extended branches, which follow Masing's criterion (Masing, 1926, as cited in Richart and Wylie, 1977), are represented by a similar equation.

For computational efficiency, recently we recast the Ramberg–Osgood equations in terms of three (G_o, R, and τ_{ref}) rather than four (G_o, α, R, and τ_y) parameters. This revision preserves the flexibility of the original equations while making quite manageable the process of establishing values for the parameters of the equations. The revised equation for the skeleton curve is

$$\gamma = \frac{\tau}{G_o}\left[1 + \left|\frac{\tau}{\tau_{ref}}\right|^{R-1}\right], \quad (2)$$

where

$$\tau_{ref} = \alpha^{-(1/(R-1))}\tau_y. \quad (3)$$

The following equation gives the normalized secant shear modulus for peak stress versus strain coordinates τ_1 and γ_1 (see Figure 3) in these new terms and may be derived from an equivalent relation given by Richart and Wylie (1977):

$$\frac{G}{G_o} = \left[1 + \left|\frac{\tau_1}{\tau_{ref}}\right|^{R-1}\right]^{-1}. \quad (4)$$

An equation that similarly gives the equivalent viscous damping ratio and that may be derived from an equivalent relation presented by Idriss *et al.* (1978) is

$$D = \frac{2}{\pi}\left(\frac{R-1}{R+1}\right)\frac{\tau_{ref}}{G_o\gamma_1}\left(\frac{\tau_1}{\tau_{ref}}\right)^R. \quad (5)$$

This equation is based on the frequently cited relation that defines an equivalent viscous damping ratio for hysteresis:

$$D = \frac{\Delta W}{2\pi G\gamma_1^2}, \quad (6)$$

where ΔW is the area within the stress versus strain curves for a single cycle of loading (Jacobsen, 1930 as cited in Idriss *et al.*, 1978). An important aspect of the damping ratio curves based on equation (5) is that they are fully and unambiguously defined by either the shear stress versus strain curves described by equation (2) or the shear modulus reduction curves obtained using equation (4).

It should be noted that the Ramberg–Osgood equations do not describe either the rounding of the reversals of stress versus strain curves observed in cyclic tests of clayey soils (Vucetic, 1990) or effects of dilation seen in cyclic tests of saturated cohesionless soils.

With respect to revisions to the procedure for establishing most representative simulations, we first automated the procedure. The automated procedure, which is based on the least squares method, largely eliminates the need for judgment and is efficient. Using the procedure, for the jth trial simulation, we compute a value for Ψ_j defined as

$$\Psi_j = \sum_{i=0}^{\eta}(\ddot{\theta}_{mi} - \ddot{\theta}_{ci})^2, \quad (7)$$

where $\ddot{\theta}_{mi}$ and $\ddot{\theta}_{ci}$ are the measured and the computed angular accelerations of the instrumented head, respectively, at the end of the ith time interval, and η = the number of time intervals. Trial simulations are repeated until the value of Ψ_j falls to a minimum for which the values of the parameters of interest satisfy specified tolerances. This establishes the most representative simulation. The values inferred for G_o, τ_{ref}, and R may then be introduced into equations (2), (4), and (5) to provide, for the tested soil, idealized descriptions of in situ nonlinear shear stress versus strain curves and corresponding shear modulus reduction and damping ratio versus strain curves. We also revised our procedure for simulating high-strain tests. Now we consider only the initial portions of tests, during which the peak strains are high, and not the decaying vibrations during the later portions of tests. These vibrations may have diluted somewhat the impacts of the high-strain portions of tests on interpretations of test results, since they generally represent substantial portions of tests and occur under largely linear conditions.

Sites and Site Conditions

The sites of interest are the I-10/La Cienega Blvd. undercrossing (I-10) in Los Angeles (Dynamic In Situ Geotechnical Testing, Inc., 1996a; Earth Mechanics, Inc., 1994) and the National Geotechnical Experimentation Sites at the University of Massachusetts (UM) in Amherst, Massachusetts (Bonus, 1995; Dynamic In Situ Geotechnical Testing, Inc., 1996a,b; Lutenegger, personal commun., 1995), on Treasure Island (TI) in the San Francisco Bay (de Alba *et al.*, 1994; de Alba and Faris, 1996; Dynamic In Situ Geotechnical Testing, Inc., 1996a), and at Auburn University (AU) in Spring Villa, Alabama (Vinson and Brown, 1997; Dynamic In Situ Geotechnical Testing, Inc., 1998). These are sites for which results from at least low-strain seismic tests are available for comparative purposes.

As indicated by Table 1, the sites cover a broad range of soil conditions relevant to earthquake engineering. These include soft to medium-stiff clays and saturated loose sands.

Sample Results

Sample test and analysis results are provided in Figures 4 and 5 for impulse shear tests carried out at each of the four sites. In each figure, we show the measured applied torque, the angular acceleration of the instrumented head as measured and as computed as part of the most representative simulation of the test, and shear stress versus strain curves described by this simulation for the tested soil. Figure 4 shows results for low-strain tests, in which the stress versus strain behaviors of the tested soils are described to be largely linear and elastic. Figure 5 shows results for high-strain tests, in which the stress versus strain behaviors of the tested soils are described to be highly nonlinear and inelastic.

In Figure 6, we show sample results that provide insight into the process of establishing most representative simulations. The figure shows an array of values of τ_{ref} and R for which we carried out trial simulations of a selected high-strain impulse shear test. Superimposed on the array are contours for selected values of Ψ_j normalized to the minimum

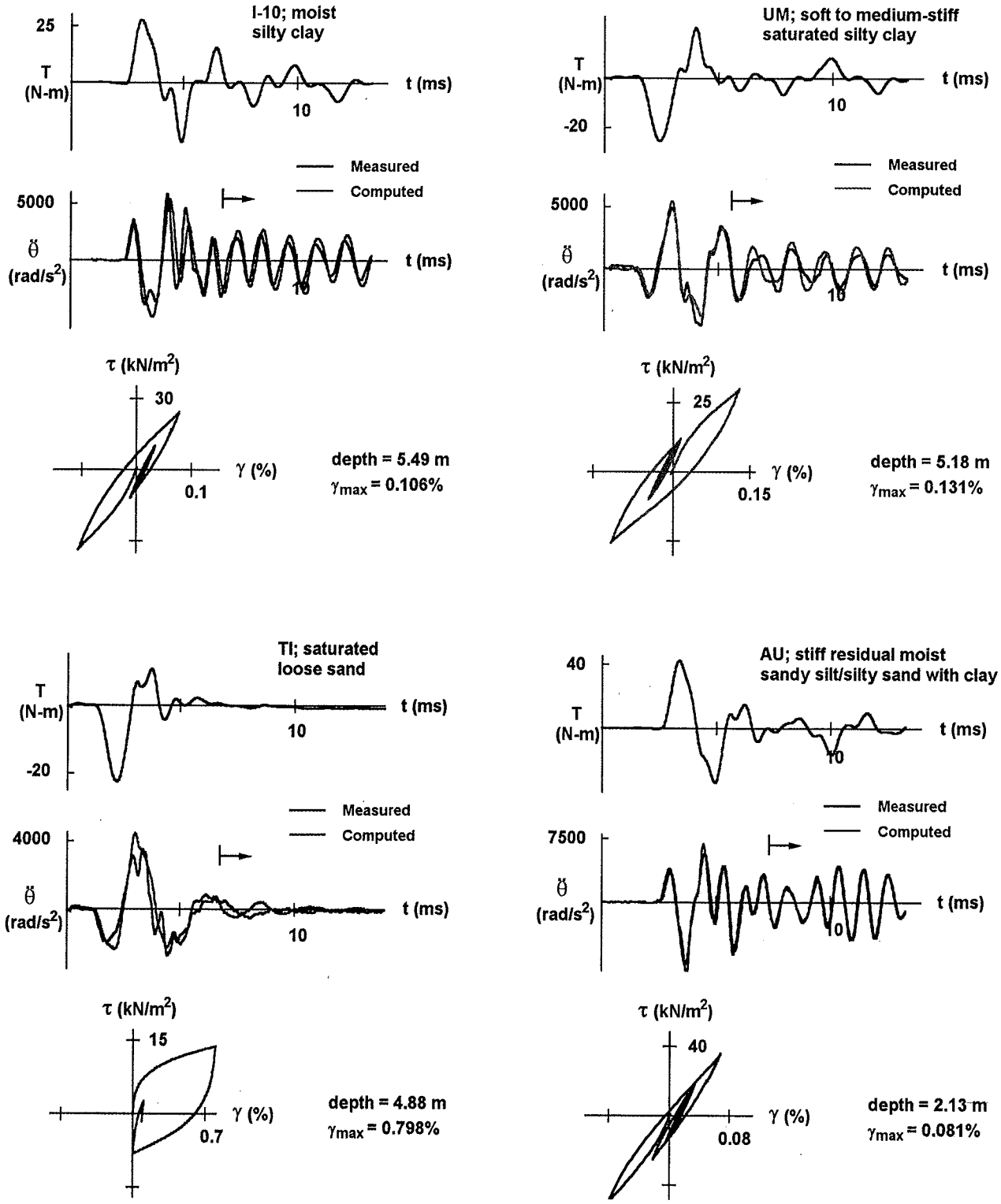

Figure 5. Sample results from high-strain impulse shear tests and corresponding most representative simulations. The stress versus strain curves were computed for the soil at the wall of the probe cylinder. The portions of the computed motion records beyond the arrows were not used in interpreting test results. The values inferred for relevant soil parameters are provided in Table 1. Abbreviations as in text.

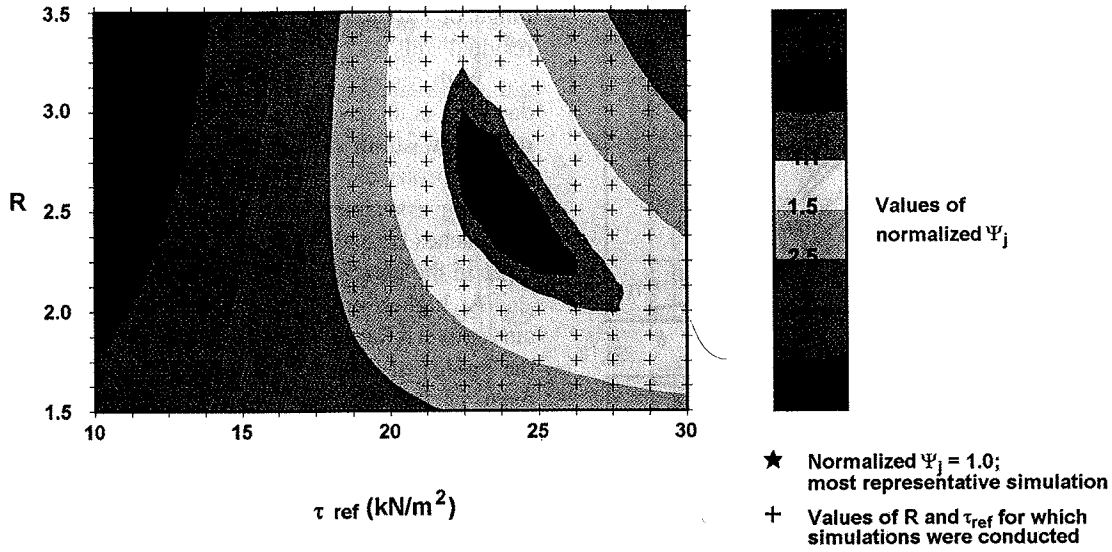

Figure 6. Sample results from trial simulations of high-strain impulse shear tests showing identification of most representative simulation. The results are for the University of Massachusetts site test represented in Fig. 5. The values of Ψ_j are normalized to the minimum value of Ψ_j.

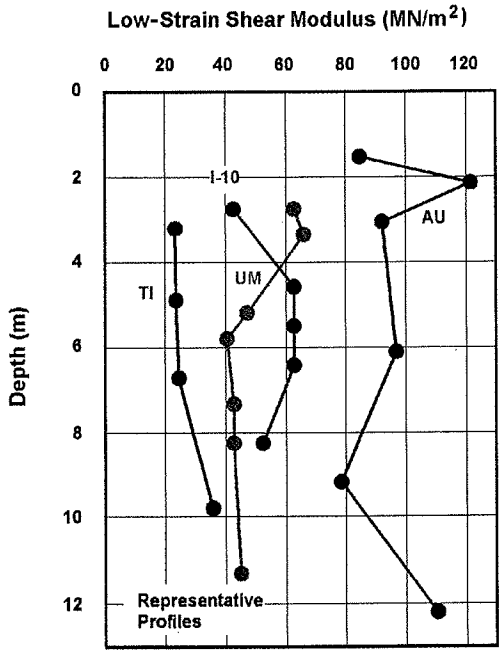

Figure 7. Low-strain shear modulus profiles inferred for the sites (abbreviations as in text).

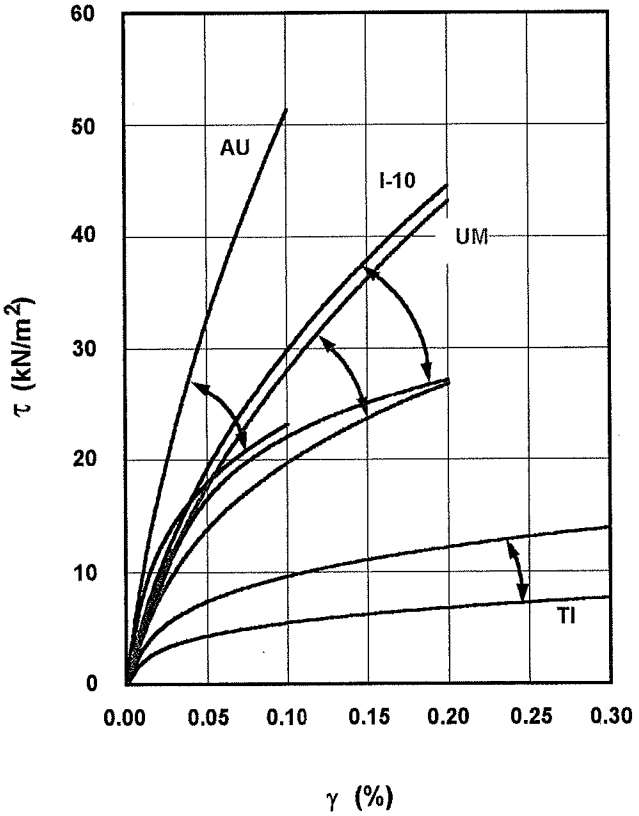

Figure 8. Ranges of idealized skeleton shear stress versus strain curves inferred for the sites (abbreviations as in text).

deposits, these agreements suggest that the impulse shear test may not have disturbed the tested soils excessively.

With respect to the comparison for the Treasure Island site (Fig. 10c), although the agreement is reasonable and the profile we inferred follows closely the trend of the profile based on seismic tests, it consistently falls somewhat below that profile. We believe that this was likely caused largely by small rises of fluid sand toward the drilling auger assem-

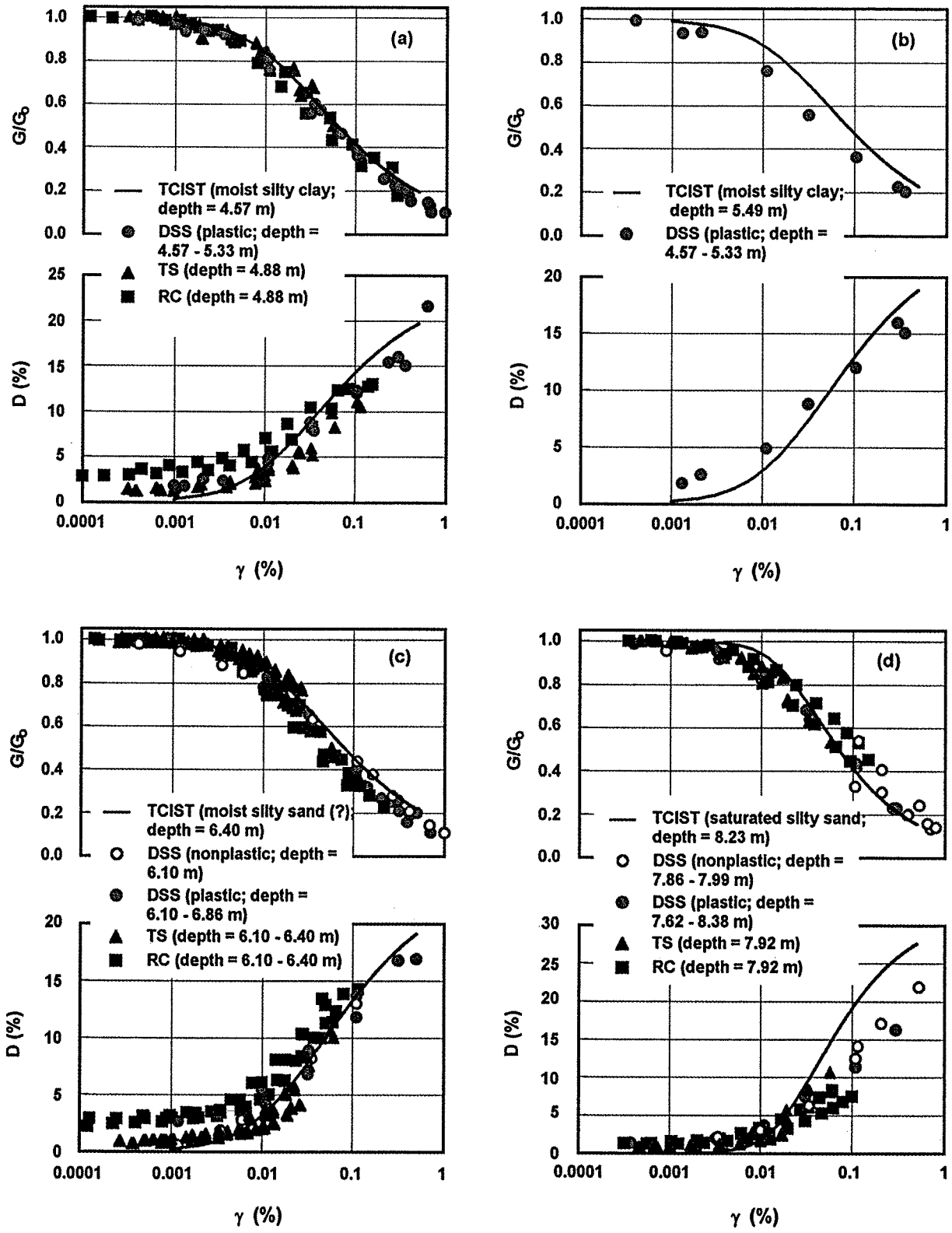

Figure 11. High-strain information inferred for the I-10/La Cienega Blvd. site from the results of impulse shear tests superimposed on results from laboratory direct simple shear tests (DSS; Vucetic *et al.*, 1998) and laboratory resonant column (RC) and torsional shear (TS) tests (Rosrine, 1998b) conducted on samples of soil recovered from the site. Other abbreviations as in text.

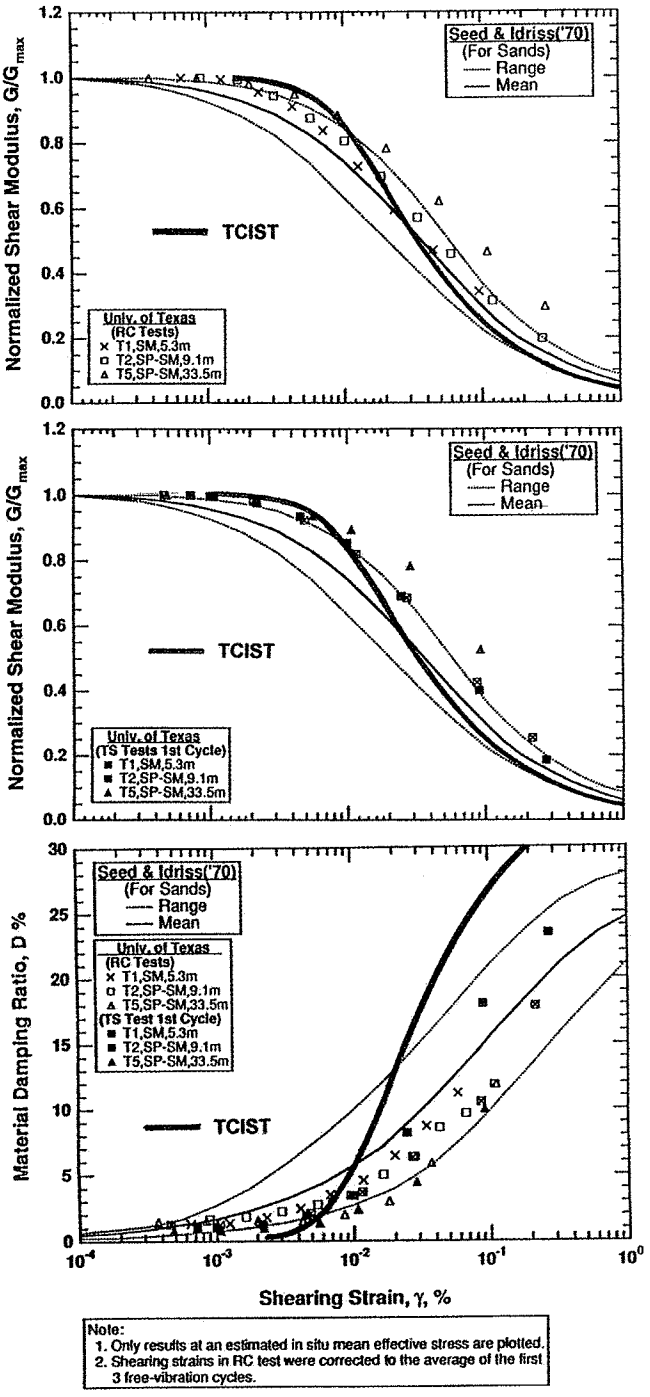

Figure 12. High-strain information inferred for the Treasure Island site (representative average curves; the individual curves on which these are based fall into narrow bands) superimposed on corresponding information published by Hwang and Stokoe (1993) and based on results of laboratory resonant column (RC) and torsional shear (TS) tests conducted on undisturbed samples of sand recovered from the site. The impulse shear tests covered the depth range of 3.2 to 9.75 m. TCIST, torsional cylindrical impulse shear test.

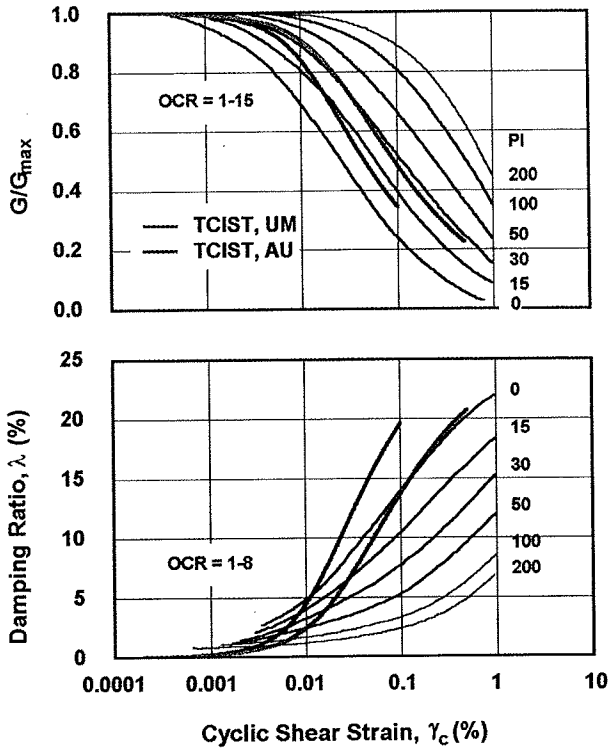

Figure 13. High-strain information inferred for the University of Massachusetts and Auburn University sites (representative average curves) superimposed on published information developed by Vucetic and Dobry (1991) and reproduced from the Rosrine (1998a) database. (The damping ratio curves in the database fall slightly below those in the 1991 publication.) The average plasticity index for the University of Massachusetts site over the depth range of 1.52 to 12.19 m was calculated to be 19.4 (FHWA, 1995; Dynamic In Situ Geotechnical Testing, Inc., 1996a,b). The average plasticity index of plastic samples taken from the Auburn University site for the depth range of 1 to 15 m was 8.2 with a standard deviation of 5.9 (based on 22 tests); 20 samples were found to be nonplastic (Vinson and Brown, 1997). Abbreviations as in text.

in Figure 11d were above the water table (depth reported to be 9.1 m) and show levels of damping comparable to those shown in Figure 11c. The representative average damping ratio curve we inferred for the Treasure Island site (Fig. 12), which was for sands and silty sands beneath the water table, behaves similarly to the damping ratio curve of Figure 11d. Porewater pressures may well have developed during the impulse shear tests conducted at the Treasure Island site. The shallow sands at this site are fairly loose and presumably saturated, and the maximum shear strains developed within the tested soils during high-strain impulse shear tests consistently were found to be particularly high (see for example, Fig. 5). Steps are now being taken toward gaining insights into effects of porewater pressures. For example, we are adding the capability to describe buildups in porewater pressure

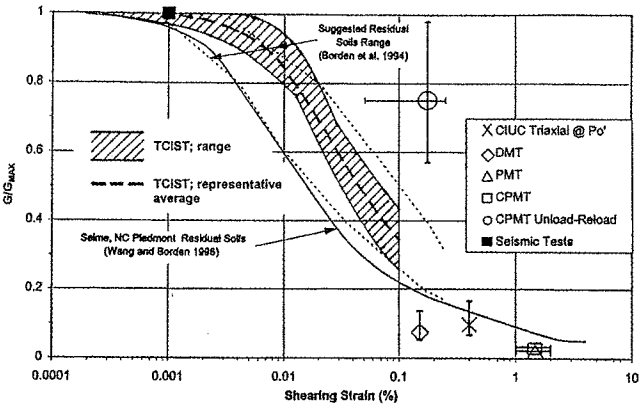

Figure 14. High-strain information inferred for the Auburn University site (range and representative average curve) superimposed on corresponding information taken from Vinson and Brown (1997). The tests listed in the legend were conducted at the site over the depth range of 3 to 12 m. CIUC, consolidated isotropically undrained triaxial test; DMT, flat dilatometer test; PMT, pressuremeter test; CPMT, cone pressuremeter test. Other abbreviations as in text.

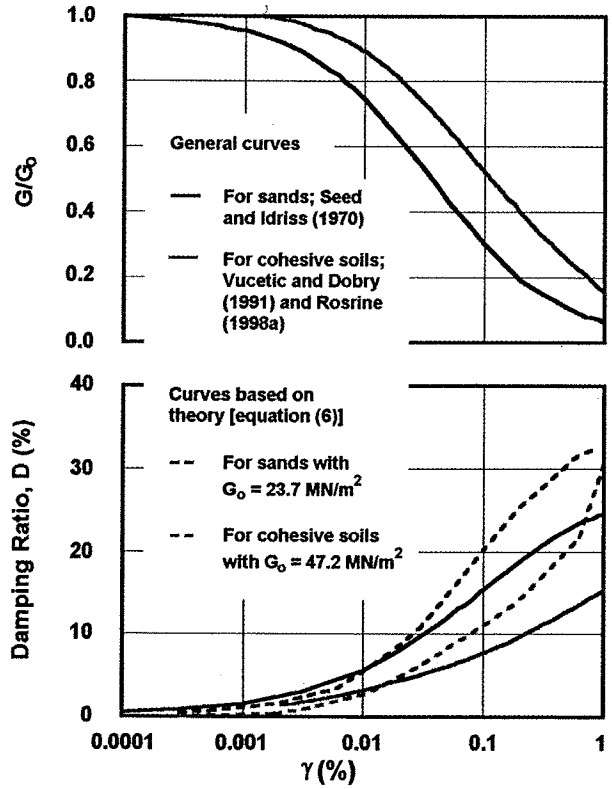

Figure 15. Comparisons between published general damping ratio curves and damping ratio curves based on theory. The general curves for sands are scaled from Fig. 12. The general curves for cohesive soils are those from Fig. 13 for the representative value of plasticity index of 30. Abbreviations as in text.

in the test soil to our procedure for simulating impulse shear tests and recently we developed, for Geo-Research Institute of Osaka, Japan, an impulse shear testing system with the capability to measure porewater pressure.

Test-related disturbances and analytical modeling may also affect damping ratios inferred for higher levels of strain. Detailed study is needed in these areas; however, as indicated previously, on the basis of our low-strain comparisons we believe that disturbances may not have been excessive.

Conclusions

This article presents preliminary field evaluations of a new in situ geotechnical test, the torsional cylindrical impulse shear test. Our findings suggest that the impulse shear test is a promising means for estimating, for a broad and relevant range of soil conditions, detailed information on in situ nonlinear inelastic shearing deformation characteristics needed for dynamic geotechnical earthquake analysis procedures used to predict ground motions and the potential for liquefaction during earthquakes. At the same time, however, uncertainties did arise in applying the impulse shear test. Areas of further research and development were identified. Several of these areas are now being addressed.

Acknowledgments

We thank the reviewers of our manuscript for their efforts and constructive comments. The testing programs summarized herein were supported by FHWA and NSF (Grant Number CMS-9416175). We greatly appreciate this support, the support provided by FHWA toward the development of the testing system used for the programs, and the efforts of A. DiMillio and C. Ealy of FHWA and C. Astill of NSF. We also thank Geo-Research Institute of Osaka, Japan, and its director, Y. Iwasaki, for providing the support that made this paper possible. Additionally, we appreciate the efforts of the many individuals involved in establishing and maintaining the National Geotechnical Experimentation Sites. Moreover, we are grateful to A. Lutenegger of the University of Massachusetts; D.A. Brown and S. Chakraborty of Auburn University; G. Mullins of the University of South Florida; R. Faris of the Naval Facilities Engineering Command; P. de Alba of the University of New Hampshire; C. Roblee, W. Cain, R. Hinton, E. Sumrow, J. Mason, and P. Porteus of Caltrans; and the fire safety officers at Treasure Island for their contributions toward the testing programs. We thank Dino, Jeff, and Juan of Gregg Drilling and Testing, Inc.; Perfecto and Jaime of HEW Drilling Company, Inc.; Steve, John, and Patrick of Connecticut Test Borings, Inc.; and Richard, Josh, and Alonzo of Christian Testing Laboratories, Inc., all of whom provided drilling services. And as always, we are grateful for the contributions of the Bechdon Company and M. Minor of this firm toward mechanical and electrical matters, and the contributions of F. Rybak of Artek Associates toward electronic matters.

References

Bonus, M. M. (1995). Comparison of recompression and SHANSEP DSS stress–strain–strength behavior of Connecticut Valley varved clay, *M.S. Thesis*, University of Massachusetts, Amherst.

Borden, R. H., L. Shao, and A. Gupta (1994). Construction related vibrations, FHWA/NC/94-007, FHWA, Washington, D.C. (as cited in Wang and Borden, 1996).

Briaud, J.-L., R. L. Lytton, and J.-T. Hung (1983). Obtaining moduli from cyclic pressuremeter tests, *J. Geotech. Eng.* **109,** no. 5, 657–665.

de Alba, P., and J. R. Faris (1996). Workshop on future research: deep instrumentation array, Treasure Island NGES, July 27, 1996: report to the workshop, current state of site characterization and instrumentation, University of New Hampshire, 45 pp.

de Alba, P., J. Benoit, D. G. Pass, J. J. Carter, T. L. Youd, and A. F. Shakal (1994). Deep instrumentation array at the Treasure Island Naval Station, in *The Loma Prieta, California, Earthquake of 17 October 1989: Strong Ground Motion, U.S. Geol. Surv. Prof. Pap. 1551-A,* 151–168.

Dynamic In Situ Geotechnical Testing, Inc. (1996a). In situ nonlinear shear stress vs strain characteristics for shallow layers of soil: I-10/La Cienega Blvd. undercrossing, Los Angeles, California, report, Lutherville, Maryland (available from author).

Dynamic In Situ Geotechnical Testing, Inc. (1996b). Operability tests of prototype simplified torsional cylindrical impulse shear testing system, report, Lutherville, Maryland (available from author).

Dynamic In Situ Geotechnical Testing, Inc. (1998). In situ low and high strain deformation characteristics for shallow layers of soil: Bayou Chico site, Pensacola, Florida and Auburn University site, Spring Villa, Alabama, report, Lutherville, Maryland (available from author).

Dynamic In Situ Geotechnical Testing, Inc. (2000). In situ nonlinear inelastic shearing deformation characteristics of soil deposits inferred using the torsional cylindrical impulse shear test, report, Lutherville, Maryland (available from author).

Earth Mechanics, Inc. (1994). Boring logs for La Cienega Blvd./Venice Blvd. undercrossing, prepared for California Department of Transportation.

Federal Highway Administration (FHWA) (1995). National Geotechnical Experimentation Sites database (software available from FHWA: Contact M. Adams, Turner-Fairbank Highway Research Center, McLean, Virginia, tel. 703-285-2161).

Henke, R., and W. Henke (1986). Method and apparatus for testing soil, U.S. Patent No. 4,594,899. International patents also exist.

Henke, R., and W. Henke (1993a). Nonlinear torsional dynamic coupled continuum–discrete parameter analysis, in *Proc. of the 1993 National Earthquake Conference*, held in Memphis, Tennessee, 2–5 May 1993, 77–86.

Henke, W., and R. Henke (1993b). Laboratory evaluation of in situ geotechnical torsional cylindrical impulse shear test for earthquake resistant design, *Bull. Seism. Soc. Am.* **83,** no. 1, 245–263.

Hwang, S. K. and K. H. Stokoe II (1993). Dynamic properties of undisturbed soil samples from Treasure Island, California, geotechnical engineering report GR93-4, University of Texas, Austin.

Idriss, I. M., R. Dobry, and R. D. Singh (1978). Nonlinear behavior of soft clays during cyclic loading, *J. Geotech. Eng.* **104,** no. 12, 1427–1447.

Jacobsen, L. (1930). Motion of a soil subjected to simple harmonic ground vibration, *Bull. Seism. Soc. Am.*, **20**.

Masing, G. (1926). Eigenspannungen und Verfestigung beim Messing, *Proc. of the Second International Congress of Applied Mechanics*, Zurich.

Richart, F. E., Jr., and E. B. Wylie (1977). Influence of dynamic soil properties on response of soil masses, in *Structural and Geotechnical Mechanics: A Volume Honoring Professor Nathan M. Newmark,* W. J. Hall (Editor), Proc. of the Symposium of Structural and Geotechnical Mechanics, Urbana, Illinois, 2–3 October 1975.

Roblee, C. J., and M. F. Riemer (1998). The downhole freestanding shear device concept, in *Geotechnical Earthquake Engineering and Soil Dynamics III,* Seattle, Washington, 3–6 August 1998, American Society of Engineers, 200–212.

Rosrine (1998a). Database, curves of Vucetic and Dobry (1991), *http://geoinfo.usc.edu/rosrine/* (last accessed June 2002).

Rosrine (1998b). Database, University of Texas, Austin, test results, *http://geoinfo.usc.edu/rosrine/* (last accessed June 2002).

Salgado, R., V. P. Drnevich, A. Ashmawy, W. P. Grant, and P. Vallenas (1997). Interpretation of large-strain seismic cross-hole tests, *J. Geotech. Geoenviron. Eng.* **123,** no. 4, 382–388.

Seed, H. B., and I. M. Idriss (1970). Soil moduli and damping factors for dynamic response analyses, EERC 70-10, Earthquake Engineering Research Center, University of California, Berkeley.

Seed, H. B., R. T. Wong, I. M. Idriss, and K. Tokimatsu (1986). Moduli and damping factors for dynamic analyses of cohesionless soils, *J. Geotech. Eng.* **112,** no. 11, 1016–1032.

Stokoe, K. H., II, S.-H. Joh, and J. A. Bay (1998). In situ v_s profiles from SASW testing at geotechnical sites shaken by the 1994 Northridge earthquake, in *Proc. of the NEHRP Conference and Workshop on Research on the Northridge, California Earthquake of January 17, 1994,* California universities for research in earthquake engineering, held in Los Angeles, California, 20–22 August, 1997, 403–412.

Vinson, J. L., and D. A. Brown (1997). Site characterization of the Spring Villa geotechnical test site and a comparison of strength and stiffness parameters for a Piedmont residual soil, report by the Highway Research Center, Harbert Engineering Center, Auburn University, Auburn, Alabama.

Vucetic, M. (1990). Normalized behavior of clay under irregular cyclic loading, *Can. Geotech. J.* **27,** 29–46.

Vucetic, M., and R. Dobry (1991). Effect of soil plasticity on cyclic response, *J. Geotech. Eng.* **117,** no. 1, 89–107.

Vucetic, M., M. Doroudian, and C.-C. Hsu (1998). Rosrine database, University of California at Los Angeles, test results, *http://geoinfo.usc.edu/rosrine/* (last accessed June 2002).

Wang, C. E. and R. H. Borden (1996). Deformation characteristics of Piedmont residual soils, *J. Geotech. Eng.* **122,** no. 10, 822–830.

Dynamic In Situ Geotechnical Testing, Inc.
7 Wyndam Court
Lutherville, Maryland 21093

Manuscript received 15 November 2000.

Appendix B: Sample Results

In this appendix, we provide samples of our test and analysis results for our 2002 testing program at the Treasure Island site. The sample results are presented in Figs. B1 through B3. These include results from low strain and moderate-load and high-load high strain impulse shear tests conducted in borehole #1 in the upper sandy layer, the sand/clay transition sublayer, and the underlying clay layer (see Fig. 8). For each test, we show the measured applied torque; the angular acceleration of the instrumented head as measured and as computed using the values inferred for the Ramberg-Osgood equation parameters from the results of the low strain (5V) and the moderate-load high strain (30 V) tests that are shown in the figures; and the computed shear stress vs strain curves for the soil at the wall of the probe cylinder.

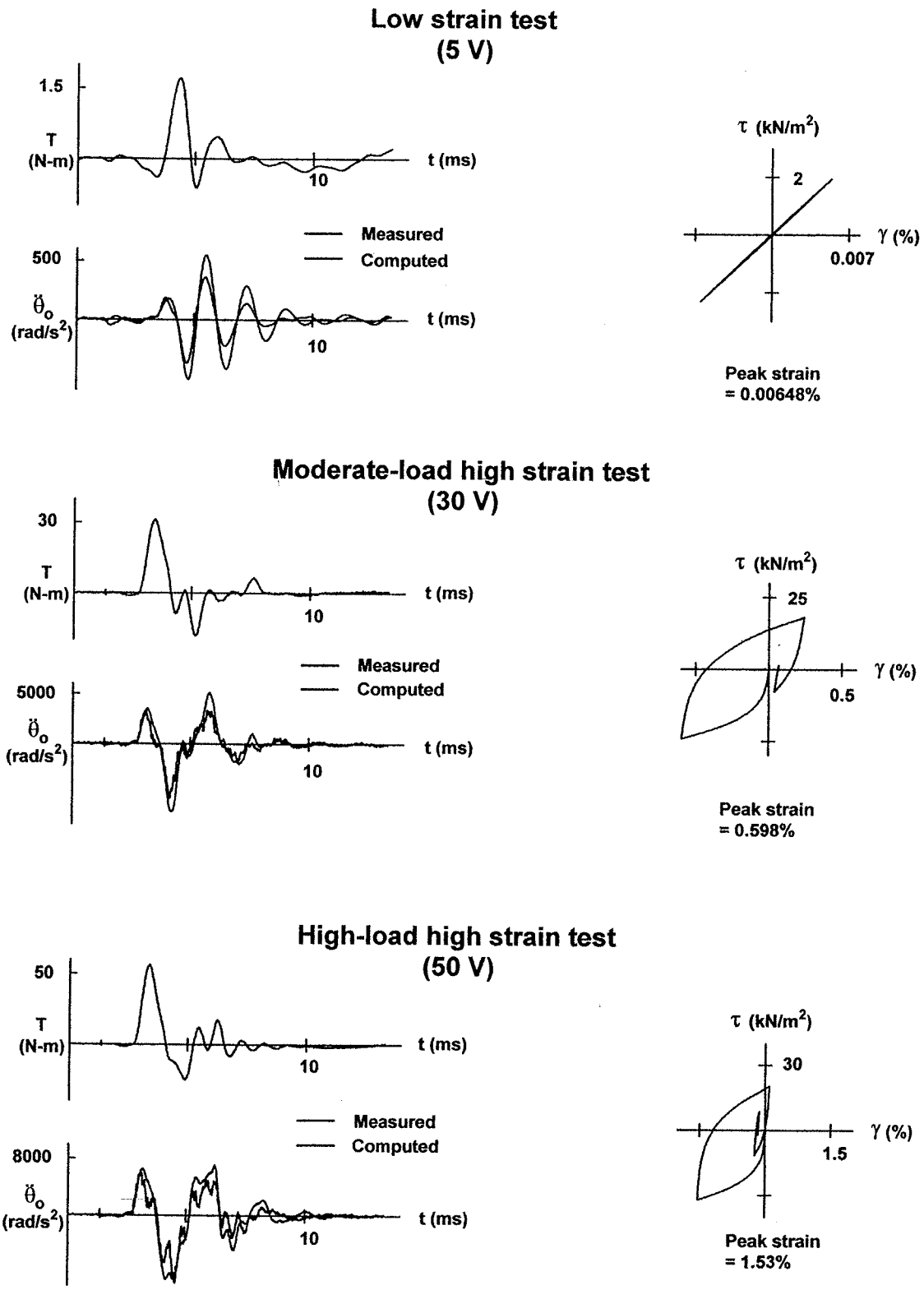

Figure B1: Results from representative impulse shear tests conducted in loose saturated clayey sandy silt at the depth of 5.18 m in borehole #1 at the Treasure Island site (2002 testing program) and from corresponding simulations.

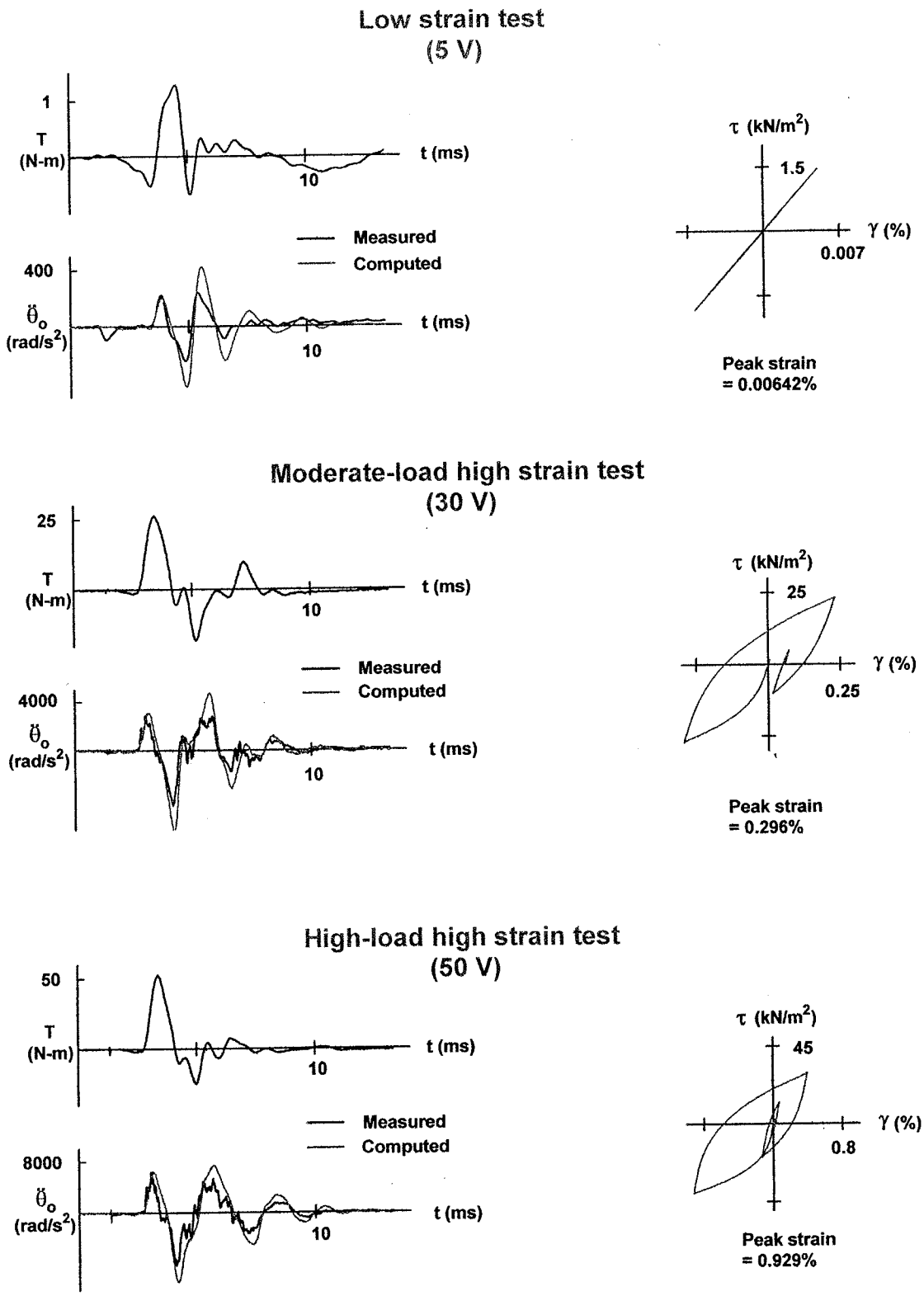

Figure B2: Results from representative impulse shear tests conducted in sand/clay transition sublayer at the depth of 12.8 m in borehole #1 at the Treasure Island site (2002 testing program) and from corresponding simulations.

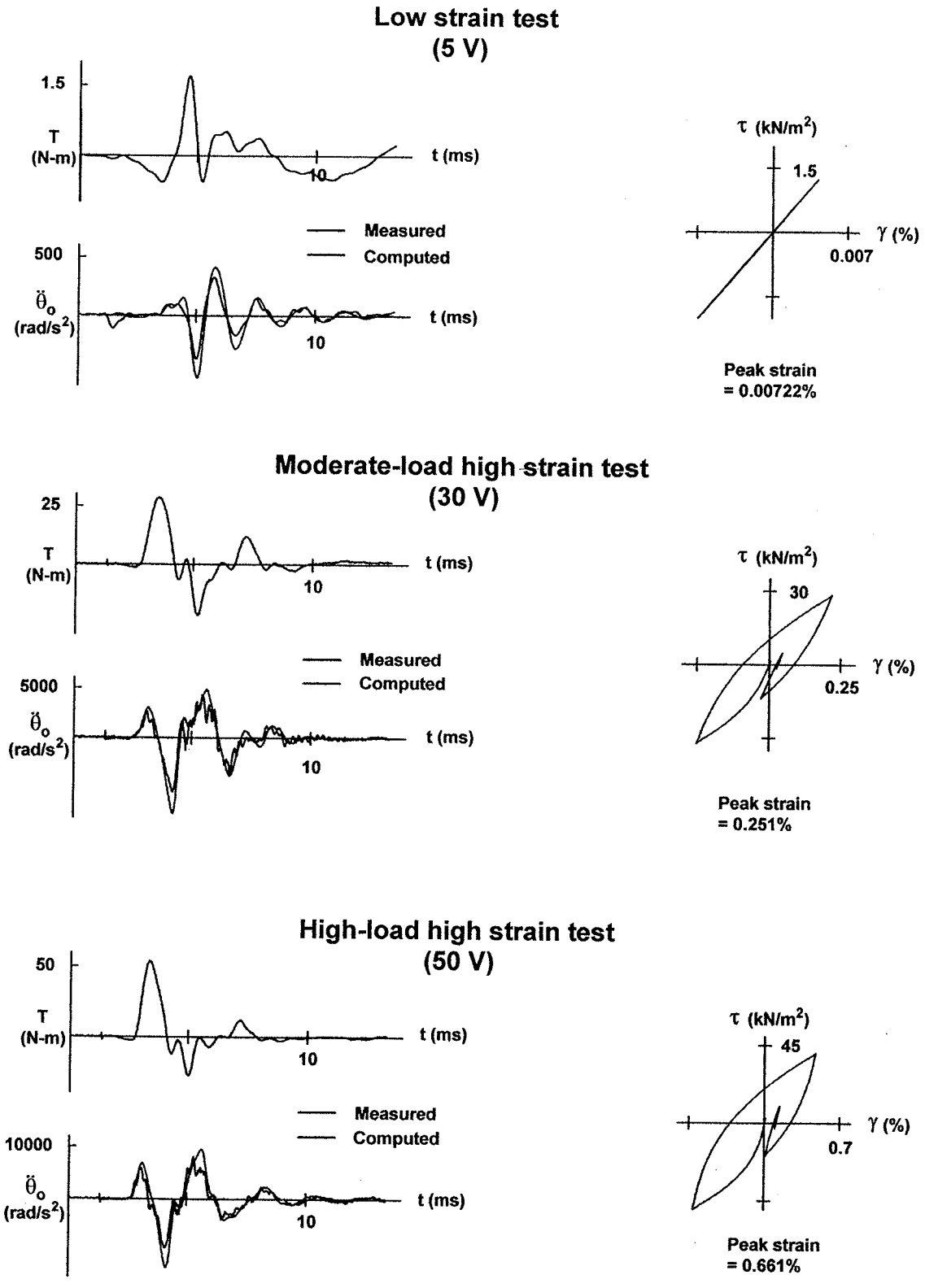

Figure B3: Results from representative impulse shear tests conducted in medium-stiff clay ("Young Bay Mud") at the depth of 18.9 m in borehole #1 at the Treasure Island site (2002 testing program) and from corresponding simulations.